[redacted] SECURITY INFORMATION

Copy 203
RM L53F24

NACA

RESEARCH MEMORANDUM

EFFECT OF REDUCTION IN THICKNESS FROM 6 TO 2 PERCENT AND REMOVAL OF THE POINTED TIPS ON THE SUBSONIC STATIC LONGITUDINAL STABILITY CHARACTERISTICS OF A 60° TRIANGULAR WING IN COMBINATION WITH A FUSELAGE

By William E. Palmer

Langley Aeronautical Laboratory
Langley Field, Va.

CLASSIFIED DOCUMENT

[redacted]

NATIONAL ADVISORY COMMITTEE
FOR AERONAUTICS

WASHINGTON

August 19, 1953

[redacted]

1L

NACA RM L53F24

[redacted]

NATIONAL ADVISORY COMMITTEE FOR AERONAUTICS

RESEARCH MEMORANDUM

EFFECT OF REDUCTION IN THICKNESS FROM 6 TO 2 PERCENT AND REMOVAL OF THE POINTED TIPS ON THE SUBSONIC STATIC LONGITUDINAL STABILITY CHARACTERISTICS OF A 60° TRIANGULAR WING IN COMBINATION WITH A FUSELAGE

By William E. Palmer

SUMMARY

A wind-tunnel investigation was conducted to determine the effects on lift, drag, and pitching moment of a reduction of the thickness ratio of a 60° triangular wing from 6 percent to 2 percent at Mach numbers from 0.15 to 0.40 and Reynolds numbers from 0.9×10^6 to 9×10^6. Investigated, in addition, were the effects of the removal of the outer 24.9 percent of the span of the 6-percent-thick wing through a range of Mach numbers from 0.40 to 0.85 at Reynolds numbers from 3×10^6 to 6×10^6. Angles of attack ranged from -4° to 36° for all tests except where limited by tunnel choke.

The results of this investigation show that either a reduction of thickness ratio or the removal of the tips produced an increase in drag due to lift, a reduction in values of maximum lift-drag ratio, and a less negative variation of pitching-moment coefficient with lift coefficient at moderate angles of attack. The variation of lift coefficient with angle of attack at zero lift was reduced by removal of the wing tips, but was not affected by the reduction of thickness. Drag due to lift was seen at low speeds to be dependent on the Reynolds number based on the wing leading-edge radius; however, at high subsonic Mach numbers, Reynolds number effects on drag due to lift decreased. Irregularities observed in the lift and pitching-moment curves of the 6-percent-thick delta wing at a lift coefficient of approximately 0.4 and Mach numbers of 0.60 to 0.85 were eliminated by the removal of the pointed tips.

INTRODUCTION

The high-strength characteristics of wings with triangular plan forms permit the use of very thin airfoil sections which provide low

[redacted]

minimum-drag characteristics at supersonic speeds. The small values of leading-edge radius associated with thin wings, however, are known to result in poor drag-due-to-lift characteristics at subsonic speeds. In order to provide quantitative information on the effects of both wing thickness and Reynolds number at subsonic speeds on the drag as well as on the lift and longitudinal stability characteristics of delta plan forms, an investigation was made in the Langley low-turbulence pressure tunnel of two delta-wing—fuselage combinations. Each configuration had a wing with leading-edge sweepback of 60°, an aspect ratio of 2.31, and a taper ratio of zero. One wing had NACA 65A006 airfoil sections and the other had NACA 65A002 airfoil sections parallel to the plane of symmetry. Tests were made through a range of angle of attack from -2° to 36° at Reynolds numbers from 0.9×10^6 to 9×10^6 and at Mach numbers from 0.15 to 0.85 for the 6-percent-thick wing and 0.15 to 0.40 for the 2-percent-thick wing. Data at higher subsonic Mach numbers for the 2-percent-thick wing are available in reference 1.

One of the problems involved in the use of thin delta wings of constant percentage thickness is the difficulty associated with construction of the pointed tips because of the very small absolute thickness of these sections. Recent (unpublished) free-flight tests of thin delta-wing models have indicated also a tendency for the tip sections to flutter. To determine, therefore, the effects on the static aerodynamic characteristics of removal of the pointed tips, tests were also made on a third wing having the airfoil sections of the 6-percent-thick wing but with the plan form modified by removal of the outer 24.9 percent of the span. The resultant plan form was one having 60° sweepback of the leading edge, an aspect ratio of 1.39, and a taper ratio of 0.249. Tests were made through a range of angle of attack from -4° to 36° at Reynolds numbers from 3×10^6 to 6×10^6 and Mach numbers from 0.40 to 0.95.

SYMBOLS

The symbols used in the present paper are defined as follows:

A	aspect ratio
b	wing span, ft
C_D	drag coefficient, D/qS
C_{D_o}	drag coefficient at zero lift
C_L	lift coefficient, L/qS

$C_{L_{max}}$	maximum lift coefficient
C_m	pitching-moment coefficient, $M_{\bar{c}/4}/qS\bar{c}$
$\bar{c}$	wing mean aerodynamic chord, $\frac{2}{S}\int_0^{b/2} c^2 dy$, ft
D	drag, lb
L	lift, lb
M	Mach number
$M_{\bar{c}/4}$	pitching moment about $0.25\bar{c}$ point, ft-lb
q	free-stream dynamic pressure, $\frac{1}{2}\rho V^2$, lb/sq ft
R	Reynolds number based on $\bar{c}$
R_r	Reynolds number based on r
r	wing leading-edge radius at the mean aerodynamic chord, ft
S	total wing area, sq ft
V	free-stream velocity, ft/sec
α	model angle of attack, deg
ρ	free-stream mass density, slugs/cu ft
$(L/D)_{max}$	maximum value of lift-drag ratio
$C_{L_{(L/D)_{max}}}$	value of C_L at which $(L/D)_{max}$ occurs
$\Delta C_D/C_L^2$	drag-due-to-lift factor, $\frac{C_D - C_{D_o}}{C_L^2}$

[redacted]

APPARATUS AND PROCEDURE

Tunnel

The tests were conducted in the Langley low-turbulence pressure tunnel described in reference 2. Independent variations in Reynolds number and Mach number can be obtained by means of variations in tunnel stagnation pressure from 1 to 10 atmospheres in air and from 1/5 to 1 atmosphere in Freon-12. Mach numbers up to tunnel choke can be obtained with the use of Freon-12 as a testing medium. All data obtained in Freon-12 were converted to equivalent air data by the methods of reference 3.

Models

Three full-span wing-fuselage configurations were investigated. The first two wings were of delta plan form with 60° sweepback of the leading edge (A = 2.31); one wing had NACA 65A006 airfoil sections and the other had NACA 65A002 airfoil sections, both parallel to the plane of symmetry. Airfoil ordinates are given in table I. The third wing was identical to the 6-percent-thick delta wing except that the outer 24.9 percent of the span was eliminated to form a wing with 60° sweepback of the leading edge, an aspect ratio of 1.39, and a taper ratio of 0.249. The tips of this wing were formed by revolution of the thickness distribution about the tip chord. Additional details of the models are given in figure 1. Figure 2 is a photograph of the clipped-tip model installed in the wind tunnel.

The 6-percent-thick delta wing was solid aluminum and the other two wings were solid steel. All wings were attached to the fuselage with the trailing edge located 27.9 inches behind the fuselage nose. In this arrangement, the quarter-chord point of the mean aerodynamic chords of the two delta wings was located adjacent to the maximum diameter of the fuselage, and that of the clipped wing was 0.4 inch forward of the maximum diameter of the fuselage.

The hollow steel fuselage, the ordinates of which are given in table I, is a body of revolution of fineness ratio 10 reduced from 12 by cutting off the rear end.

Each model was sting-mounted in the tunnel as shown in figure 2. Force and moment measurements were taken by use of an electrical-type strain-gage balance housed within the model fuselage.

Tests

Tests were made through an angle-of-attack range of approximately -4° to 36°. The Reynolds numbers and Mach numbers investigated for each configuration are shown in figure 3. Points in this figure are divided into

groups in order to define more clearly the range of comparison. Groups 1 and 2 represent data that show the Mach number effects at two Reynolds numbers for the 6-percent-thick delta wing. Tests of groups 3 and 4 show the Reynolds number effects at two Mach numbers for the 2-percent-thick delta wing. Group 5 represents tests that show the effects of reducing the thickness through the Reynolds number and low Mach number range. Data represented by groups 2 and 6 show the effects of removing the pointed wing tips through the Mach number range investigated. Tests at Mach numbers greater than 0.4 were made in Freon-12.

Lift, drag, and pitching-moment were obtained at each test condition. Accuracies of the associated coefficients are estimated to be approximately ±0.01, ±0.001, and ±0.003, respectively, for most of the test data; however, the random errors for the lowest Reynolds numbers, and correspondingly low dynamic pressures, are approximately twice as large. The accuracy of the angle-of-attack mechanism has been found to be approximately ±0.1° in the most inaccurate condition.

Calculations based on static loadings indicate that for the thinnest wing at maximum lift the angular deflection resulting from aerodynamic loads is less than 0.2°. It is concluded, therefore, that aeroelastic effects on all wings tested are negligible.

Corrections

The effects on Mach number and dynamic pressure of constriction of the flow by the tunnel walls were taken into account by a method based on information presented in references 4 and 5. Angles of attack and drag coefficients were corrected for the effects of boundary-induced upwash by the method of reference 6. Angles of attack have also been corrected for support deflection resulting from load.

Because the balance system was an internal one, no forces were measured on the support sting, and the only aerodynamic tares were due to the interference effect of the sting support on the model. An investigation of the sting tares made for the present configuration and the results of reference 7 indicate that for low angles of attack the only measurable effect of the sting on the model characteristics was on the drag. At high angles of attack, however, the sting can affect the lift and pitch as well as the drag. Because of load limitations of the sting-tare arrangement, sting tares at high angles of attack have not been obtained. In an effort to avoid these unknown sting tares, fuselage-alone data from reference 8 have been algebraically subtracted from the basic wing-fuselage data, thereby leaving lift, drag, and pitching-moment coefficients of the wing plus interference. The percentage change in drag coefficient that results from the increment in base pressure due to installation of the wing on the fuselage was found to be negligible.

In order to provide quantitative information on drag due to lift and maximum lift-drag ratios for the wing-fuselage configurations investigated, the drag data were adjusted to a condition at which the static pressure at the fuselage base was equal to free-stream static pressure. All plots of drag due to lift and maximum lift-drag ratio presented herein represent data that have been adjusted to this condition.

RESULTS

Data showing the effects of reducing the wing thickness and of removing the pointed tips have been presented separately for convenience. The data are presented as indicated in the following table:

	Figures
Effect of reducing the thickness:	
Basic data	4 to 6
Lift-curve slope	7
Maximum lift coefficient	8
Static-stability parameter	9
Drag due to lift	10
Maximum lift-drag ratio	11
Effect of removing the tips:	
Basic data	12
Lift-curve slope	13
Static-stability parameter	14
Drag due to lift	15
Maximum lift-drag ratio	16

In the following discussion, any reference to a wing will pertain to the wing plus interference. The pitching-moment coefficients presented for the three wing configurations are referred to the quarter-chord point of their respective mean aerodynamic chords.

DISCUSSION

Several investigations have been made of the nature of the air flow about swept wings having small leading-edge radii (refs. 9 and 10, for example). It is believed that a brief review of some of the more important results of these studies will aid in the interpretation of the results obtained during the present investigation.

It has been shown that, for airfoil sections or wings having small leading-edge radii, the flow is characterized by a separation at the leading edge, beginning at low angles of attack, and the separated flow generally reattaches to form a "bubble." The magnitude of this separation bubble is markedly affected by leading-edge radius and Reynolds number and increases with a decrease in either parameter. For wings swept back more than approximately 35°, the separated flow tends to coalesce toward the tip, resulting in the formation of a cone-shaped vortex, the core of which lies along a line passing through the leading edge at the root chord and is swept back slightly more than the wing leading edge. As the angle of attack is increased, the size of the separation vortex and the sweep angle of the vortex core increase, the rate of increase being greatest at low angles.

The separation bubble reduces the leading-edge pressure peak, and if it extends over only a portion of the chord, the upper surface pressures become more negative in the region of the bubble behind the immediate vicinity of the leading edge. The net result is to increase the lift and move the section center of pressure to the rear as compared with the condition where no leading-edge separation exists. This effect has many times been described as a camber effect. Reduction of the pressure peak and increase in lift combine to produce greater drag. When the vortex cone angle increases sufficiently, the rear extremity of the separation bubble passes off the tailing edge of the tip chord and the tip section experiences complete separation and corresponding loss of lift. As the angle of attack is increased further, the cone angle continues to increase so that the inboard boundary of the completely separated region moves toward the wing root. With these facts in mind, it can be seen that changes in the aerodynamic characteristics due to certain changes in wing parameters can be related to the effects of the vortex formation over the wing.

Effects of Thickness

Lift characteristics.- Presence of the vortex-type flow is indicated in figures 4(a), 5(a), and 6(a) by the increase in lift-curve slope at a lift coefficient of approximately 0.1 for the thinner wing and at higher lift coefficients for the thicker wing as would be expected because of its larger leading-edge radius. After the initial increase in slope, the lift curves are roughly parallel up to the approach of stall (fig. 6(a)), indicating that the progress of the vortex over the mid-semispan sections is about the same for the two wings. As seen from figures 4(a), 5(a), 6(a), and 7, the effects on lift of increasing the Reynolds number from approximately 1×10^6 to 9×10^6 are, in general, small for angles of attack below wing stall.

[redacted]

The lift-curve slopes at zero lift and low speeds are approximately the same for both wing thicknesses through the range of Reynolds number investigated (fig. 7). Data of this report and those of reference 1 indicate that the lift-curve slopes at zero lift increase at the higher Mach numbers, the increase being slightly greater than that predicted by theory (ref. 11).

The slight irregularity in the lift curve of the 6-percent-thick wing at a lift coefficient of about 0.4 and Mach numbers of 0.6 to 0.85 (fig. 4(a)) is also apparent in the data for the 2-percent-thick wing as reported in reference 1. Discussion of the probable flow phenomena associated with this irregularity is presented in the section on pitching moment.

At low Mach numbers ($M < 0.3$), values of $C_{L_{max}}$ increase for the 6-percent-thick wing from 1.10 to 1.20 as the Reynolds number is increased from 1.6×10^6 to 9.3×10^6 (fig. 8(a)). Although the variation of $C_{L_{max}}$ with R is somewhat erratic for the 2-percent-thick wing, figure 8 indicates a tendency for the values of $C_{L_{max}}$ to be higher for the 2-percent-thick wing than for the 6-percent-thick wing at Reynolds numbers less than 2×10^6 and lower at Reynolds numbers greater than 2×10^6. Both wings indicate a decrease in $C_{L_{max}}$ with increase in Mach number (fig. 8(b)).

Pitching-moment characteristics.- The pitching-moment data in figures 4(b), 5(b), and 6(b) show a forward shift in aerodynamic-center position at values of C_L at which the increase in lift-curve slope was apparent. The previous discussion of the effects of the vortex flow shows that two changes in loading take place on the wing which produce opposing effects on the aerodynamic-center location: (1) the camber effect, which results in a rearward shift in section loading, and (2) the loss of lift at the tip sections as the vortex moves inboard. It is obvious from the data of figures 4(b), 5(b), and 6(b) that the tip separation has a more pronounced effect on the pitching moments even though the camber effect is sufficient to cause an increase in lift-curve slope. As would be expected, the shift in aerodynamic center begins at a lower angle of attack on the thinner wing.

At Mach numbers above 0.6, the forward movement in aerodynamic-center position for the 6-percent-thick wing becomes much more rapid with increasing lift coefficient at a lift coefficient of approximately 0.4 (fig. 4(b)). This irregularity in the pitching-moment characteristics was also noted in reference 1 for the 2-percent-thick wing and is possibly associated with an increased severity in tip stall

resulting from shock formations. Support of the assumption that stalling of the tips is the cause of the pitch variation can be obtained from figure 4(a), which indicates a decrease in lift-curve slope at the same Mach numbers and lift coefficients, and from the characteristics of the wing with the tips removed as presented in a later section. The data of figures 4(a) and 4(b) and of reference 1 also indicate that the irregularity in pitching-moment characteristics decreases in magnitude as the Mach number is increased above about 0.80.

A comparison of the curves of figure 5(b) shows that the pitching characteristics of the 2-percent-thick wing were not appreciably affected by increasing the Reynolds number from 1.8×10^6 to 9.1×10^6. As the Reynolds number is decreased to 0.9×10^6, however, the pitching-moment slope is more nearly linear at low and moderate lift coefficients and is less negative in the low-lift range (fig. 9(a)).

For the 6-percent-thick wing, figure 9(a) indicates that there is no measurable scale effect on the pitching-moment slope at zero lift. Figure 6(b) shows that for the thicker wing the initial shift in aerodynamic-center position occurs at approximately the same lift coefficient through the Reynolds number range, but the shift is more gradual at higher Reynolds numbers. Values of pitching-moment-curve slopes at zero lift are shown in figure 9 to be slightly less negative for the thinner wing through the Mach number and Reynolds number ranges tested. Data of the present report and those of reference 1 show that for both the 6- and 2-percent-thick wings the pitching-moment-curve slopes become increasingly negative at the higher subsonic Mach numbers.

Drag characteristics.- Although at Mach numbers less than 0.4 both wings had approximately the same value of drag coefficient at zero lift, the 6-percent-thick wing and wing-fuselage combination had lower drag than the 2-percent wing and combination at low and moderate lift coefficients (figs. 6(c) and 6(d)). This difference in drag at lifting conditions is attributed to the fact that the leading-edge separation occurs at a lower angle of attack, or is more extensive, for the 2-percent-thick wing. As a result of this increase in separation, less leading-edge suction is realized and the drag due to lift is greater.

In order to correlate the separation drag in terms of sharpness of the leading edge, the drag-due-to-lift factor $\Delta C_D / C_L^2$ for the wing-fuselage configuration is plotted against Reynolds number based on the wing leading-edge radius in figure 10. This figure shows that at lift coefficients of 0.2 and 0.3, the drag due to lift at low speeds is primarily dependent on the leading-edge Reynolds number, decreasing from a value of approximately 0.4 at a leading-edge Reynolds number R_r of 300

to approximately 0.22 at a value of R_r of 14,000. An increase in R_r to 21,400 produced only a small further decrease in $\Delta C_D/C_L^2$. Figure 10 shows also that at the higher subsonic Mach numbers, the rate of change of $\Delta C_D/C_L^2$ with R_r is less than that indicated at the lowest Mach numbers investigated. These drag-due-to-lift data and those of other investigations of delta-wing—body combinations have been assembled in reference 12 to show that R_r is a primary factor governing $\Delta C_D/C_L^2$ at Mach numbers less than 0.25 but that Reynolds number effects on $\Delta C_D/C_L^2$ decrease considerably with increasing Mach number.

Maximum values of lift-drag ratio for the wing-fuselage configurations are considerably lower with the 2-percent-thick wing than with the 6-percent-thick wing through the range of Reynolds number at Mach numbers less than 0.4, the difference being approximately 28 percent of the higher value (fig. 11). This difference is a result of the higher values of drag due to lift shown previously for the thinner wing. For the configuration having the 6-percent-thick wing, values of $(L/D)_{max}$ varied approximately 10 percent through the range of Mach number investigated. The lift coefficient at which $(L/D)_{max}$ occurs for both thicknesses is about 0.15 throughout the range of tests.

Effect of Removing the Wing Tips

Lift characteristics.- Removal of the outer 24.9 percent of the span reduced the lift-curve slope up to angles of attack of approximately 4° through the range of comparison (fig. 12(a)). Figure 13 shows that the reduction in $dC_L/d\alpha$ at zero lift is approximately that predicted by theory (ref. 11) and is maintained through the Mach number range tested.

At lift coefficients of 0.10 to 0.15 the formation of the separation vortex is indicated by the sudden increase in lift-curve slope for the clipped-tip wing (fig. 12(a)). In the case of the basic wing, however, the increase in slope is not realized at this low lift coefficient because the vortex is moving inboard and the tip sections lose effectiveness, thereby offsetting some of the increase in lift due to the camber effect. As α increases, the chordwise extent of the separation bubble increases until the entire tip chord of the clipped wing is covered by the bubble. At this point, the loading on the clipped wing is probably similar to that on the complete delta wing. A further increase in α then results in the same variation of lift coefficient with angle of attack for both wings.

[redacted]

It should be mentioned that for wings of aspect ratio as low as that of the clipped wing investigated (A = 1.39), increases in lift-curve slope are possible without the existence of the separation vortex (see, for example, ref. 13). Several investigators have suggested that this nonlinearity may be represented by a term of the form $a\alpha^2$, which would indicate a gradual increase of $dC_L/d\alpha$ with α. Inasmuch as the increase in lift-curve slope realized by the clipped wing at a lift coefficient of about 0.1 is rather abrupt, it is believed that this change in $dC_L/d\alpha$ is due to the separation vortex rather than to effects of low aspect ratio.

The breaks previously noted in the full-delta wing data at a lift coefficient of approximately 0.4 and Mach numbers of 0.60 to 0.85 do not appear in the curves of the clipped wing. Values of maximum lift coefficient for the two wings are about the same and occur at about the same angle of attack.

Pitching-moment characteristics.- Analysis of the curves of figure 12(b) shows that clipping the tips moved the aerodynamic center forward at low lift coefficients $0 < C_L < 0.4$. This is the result of removing a quantity of lifting surface behind the wing aerodynamic center in the range of lift coefficients where the tips of the full-delta wing are carrying load. The initial effect of the vortex flow on the clipped wing is to cause a rearward shift in aerodynamic center as a result of the increased camber effect over the outboard sections. The initial effect on the complete delta wing, on the other hand, is to produce a forward shift in aerodynamic center resulting from the more predominant tip-stall effect as previously discussed. At lift coefficients above about 0.6 the pitching-moment slopes of the two wings are nearly the same, a further indication that the inboard progress of the vortex is probably the same for both wings at the higher angles of attack.

Figure 14 shows that removal of the tips produced a positive increment in dC_m/dC_L of approximately 0.11 as compared with 0.07 predicted by theory at zero lift through the range of Mach numbers from 0.4 to 0.85. Both wings exhibit a rearward shift in aerodynamic center at the highest test Mach numbers.

Removal of the tips eliminated the sudden forward movements in aerodynamic center at Mach numbers between 0.60 and 0.85 (fig. 12(b)) as well as the decrease in lift-curve slope previously noted in figure 12(a).

Drag characteristics.- The drag coefficients are seen in figures 12(c) and 12(d) to be higher for the clipped wing at all moderate lift coefficients. Because the drag values at zero lift are virtually

[redacted]

the same for the two wings, this difference in drag due to lift can be attributed to the decreased aspect ratio. Figure 15 shows that at a lift coefficient of 0.2, clipping the tips increased the value of the drag-due-to-lift factor $\Delta C_D/C_L^2$ of the complete configuration by approximately 0.1. Consideration of the experimental values of $\Delta C_D/C_L^2$ for the two wings and the theoretical values of $\Delta C_D/C_L^2$ for zero leading-edge suction $\left(\frac{1}{57.3\frac{\partial C_L}{\partial \alpha}}\right)$ and full leading-edge suction $(1/\pi A)$ indicates that the clipped wing experiences a slightly greater proportion of the theoretical leading-edge suction than does the full-delta wing.

As a result of the increased drag due to lift and the previously mentioned decrease in lift-curve slope, removing the pointed tips reduced the maximum value of lift-drag ratio of the wing-fuselage combination on the order of 20 percent through the Mach number range tested (fig. 16). The lift coefficient at which $(L/D)_{max}$ occurs is approximately 0.15 for both wings.

SUMMARY OF RESULTS

An investigation was made to determine the effects of a reduction in thickness ratio from 6 percent to 2 percent and of the removal of the outer 24.9 percent of the span of a 60° delta-wing—fuselage configuration. This investigation produced the following results.

1. Reduction of thickness ratio at Mach numbers from 0.15 to 0.40 and Reynolds numbers from 0.9×10^6 to 9×10^6

   (a) Produced no change in the variation of lift coefficient with angle of attack $dC_L/d\alpha$ at zero lift, but increased the value of $dC_L/d\alpha$ at moderate lift coefficients

   (b) Produced a more forward location of the aerodynamic center at low and moderate angles of attack

   (c) Increased the drag due to lift at low and moderate lift coefficients

   (d) Reduced the maximum lift-drag ratio approximately 28 percent

(e) Resulted in higher values of maximum lift coefficient at Reynolds numbers less than 2×10^6 and lower values at Reynolds numbers greater than 2×10^6

2. Removal of the pointed tips of the 6-percent-thick wing at Mach numbers from 0.4 to 0.85 and Reynolds numbers of 3×10^6 to 6×10^6

(a) Reduced the value of $dC_L/d\alpha$ at low lift coefficients

(b) Produced a positive increment in rate of change of pitching-moment coefficient with lift coefficient of approximately 0.11 at zero lift

(c) Increased the drag due to lift

(d) Reduced the maximum lift-drag ratio approximately 23 percent

(e) Had little effect on the values of maximum lift coefficient at Mach numbers less than 0.80

(f) Eliminated irregularities in the lift and pitching-moment characteristics of the full-delta wing at a lift coefficient of 0.4 and Mach numbers of 0.60 to 0.85

3. Drag due to lift of the complete-delta-wing configurations at low speed was shown to decrease as the Reynolds number based on the wing leading-edge radius increased. At high subsonic Mach numbers, Reynolds number effects on drag due to lift decreased.

Langley Aeronautical Laboratory,
National Advisory Committee for Aeronautics,
Langley Field, Va., June 15, 1953.

[redacted]

REFERENCES

1. Kelly, Thomas C.: Transonic Wind-Tunnel Investigation of the Aerodynamic Characteristics of a 60° Triangular Wing in Combination With a Systematic Series of Three Bodies. NACA RM L52L22a, 1953.

2. Von Doenhoff, Albert E., and Abbott, Frank T., Jr.: The Langley Two-Dimensional Low-Turbulence Pressure Tunnel. NACA TN 1283, 1947.

3. Von Doenhoff, Albert E., and Braslow, Albert L.: Studies of the Use of Freon-12 As a Testing Medium in the Langley Low-Turbulence Pressure Tunnel. NACA RM L51I11, 1951.

4. Herriot, John G.: Blockage Corrections for Three-Dimensional-Flow Closed-Throat Wind Tunnels, With Consideration of the Effect of Compressibility. NACA Rep. 995, 1950. (Supersedes NACA RM A7B28)

5. Glauert, H.: Wind Tunnel Interference on Wings, Bodies and Airscrews. R. & M. No. 1566, British A.R.C., 1933.

6. Katzoff, S., and Hannah, Margery E.: Calculation of Tunnel-Induced Upwash Velocities for Swept and Yawed Wings. NACA TN 1748, 1948.

7. Osborne, Robert S.: High-Speed Wind-Tunnel Investigation of the Longitudinal Stability and Control Characteristics of a $\frac{1}{16}$-Scale Model of the D-558-2 Research Airplane at High Subsonic Mach Numbers and at a Mach Number of 1.2. NACA RM L9C04, 1949.

8. Osborne, Robert S., and Mugler, John P., Jr.: Aerodynamic Characteristics of a 45° Sweptback Wing-Fuselage Combination and the Fuselage Alone Obtained in the Langley 8-Foot Transonic Tunnel. NACA RM L52E14, 1952.

9. Anderson, Adrien E.: Chordwise and Spanwise Loadings Measured at Low Speed on Large Triangular Wings. NACA RM A9B17, 1949.

10. Wilson, Herbert A., Jr., and Lovell, J. Calvin: Full-Scale Investigation of the Maximum Lift and Flow Characteristics of an Airplane Having Approximately Triangular Plan Form. NACA RM L6K20, 1947.

11. DeYoung, John: Theoretical Additional Span Loading Characteristics of Wings With Arbitrary Sweep, Aspect Ratio, and Taper Ratio. NACA TN 1491, 1947.

12. Osborne, Robert S., and Kelly, Thomas C.: A Note on the Drag Due to Lift of Delta Wings at Mach Numbers up to 2.0. NACA RM L53A16a, 1953.

13. Flax, A. H., and Lawrence, H. R.: The Aerodynamics of Low-Aspect-Ratio Wings and Wing-Body Combinations. Rep. No. CAL-37, Cornell Aero. Lab., Inc., Sept. 1951.

[redacted]

TABLE I

AIRFOIL AND FUSELAGE ORDINATES

Airfoils

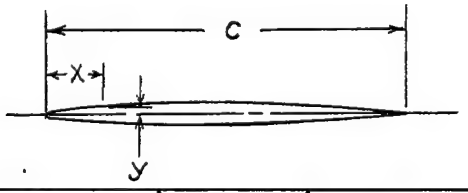

	NACA 65A006	NACA 65A002
x/c	y/c	y/c
0	0	0
.005	.00464	.00156
.0075	.00563	.00190
.0125	.00718	.00242
.025	.00981	.00329
.050	.01313	.00439
.075	.01591	.00531
.10	.01824	.00608
.15	.02194	.00731
.20	.02474	.00824
.25	.02687	.00895
.30	.02842	.00947
.35	.02945	.00981
.40	.02996	.00998
.45	.02992	.00997
.50	.02925	.00977
.55	.02793	.00936
.60	.02602	.00874
.65	.02364	.00796
.70	.02087	.00704
.75	.01775	.00601
.80	.01437	.00488
.85	.01083	.00369
.90	.00727	.00247
.95	.00370	.00126
1.00	.00013	.00005
L.E. radius =	0.00229c	.000255c
T.E. radius =	0.00014c	.000045c

Fuselage

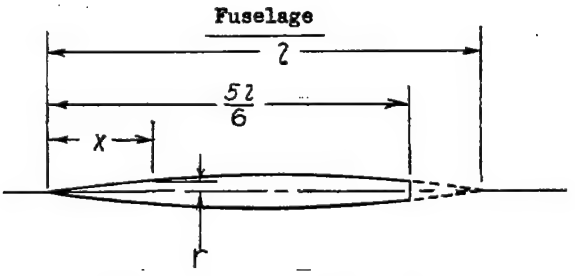

ORDINATES	
x/l	r/l
0.0050	0.00231
.0075	.00298
.0125	.00428
.0250	.00722
.0500	.01205
.0750	.01613
.1000	.01971
.1500	.02593
.2000	.03090
.2500	.03465
.3000	.03741
.3500	.03933
.4000	.04063
.4500	.04143
.5000	.04167
.5500	.04130
.6000	.04024
.6500	.03842
.7000	.03562
.7500	.03128
.8000	.02526
.8333	.02083
.8500	.01852
.9000	.01125
.9500	.00439
1.0000	0
Nose radius = 0.00052l	

NACA

[redacted]

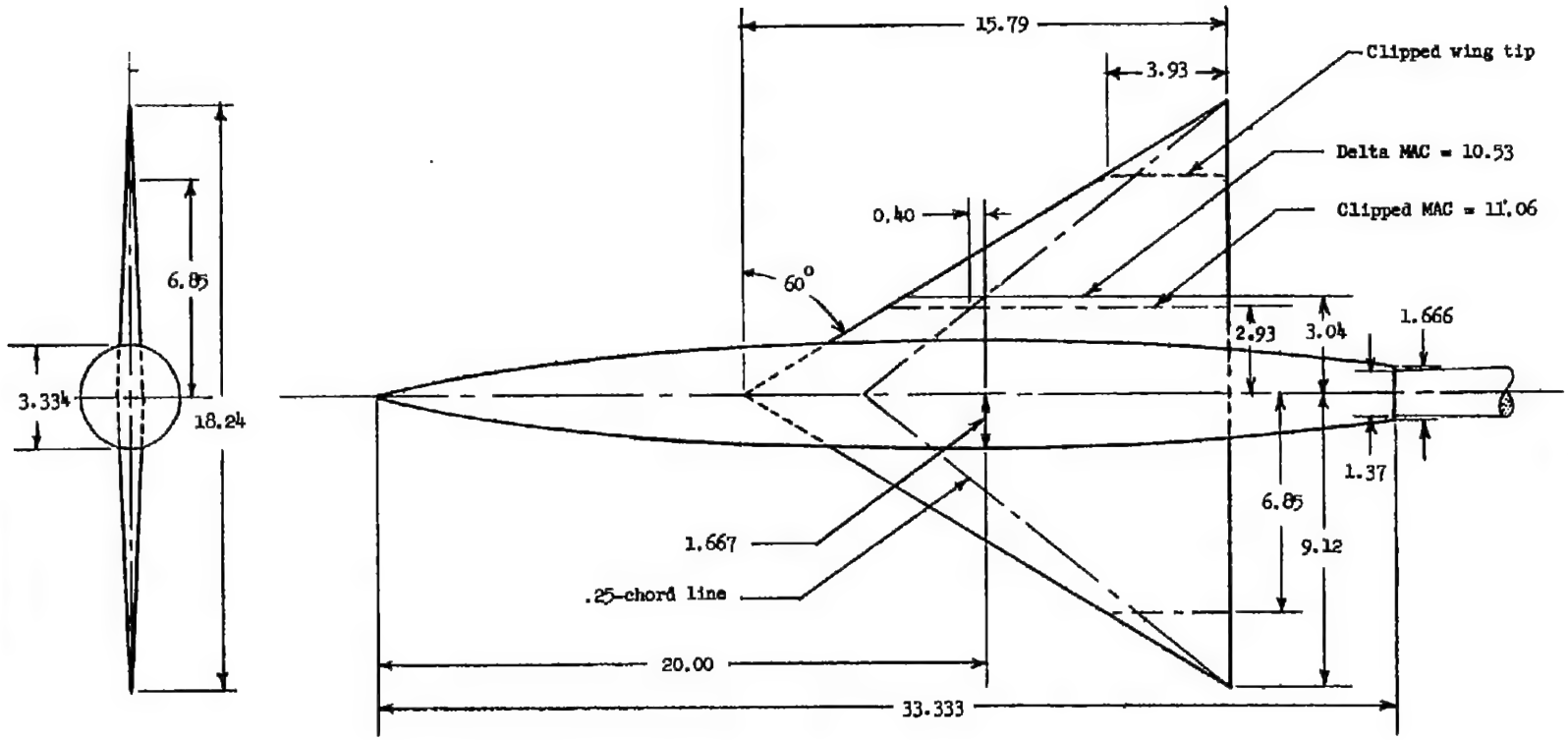

Wing	6-percent delta	2-percent delta	6-percent clipped
Airfoil section parallel to airstream	NACA 65A006	NACA 65A002	NACA 65A006
Area, sq ft	1	1	0.937
MAC, in.	10.53	10.53	11.06
Sweepback (c/4), deg	52.4	52.4	52.4
Aspect ratio	2.31	2.31	1.39
Taper ratio	0	0	0.249

Figure 1.- Details of the wing-fuselage configurations. All dimensions are in inches.

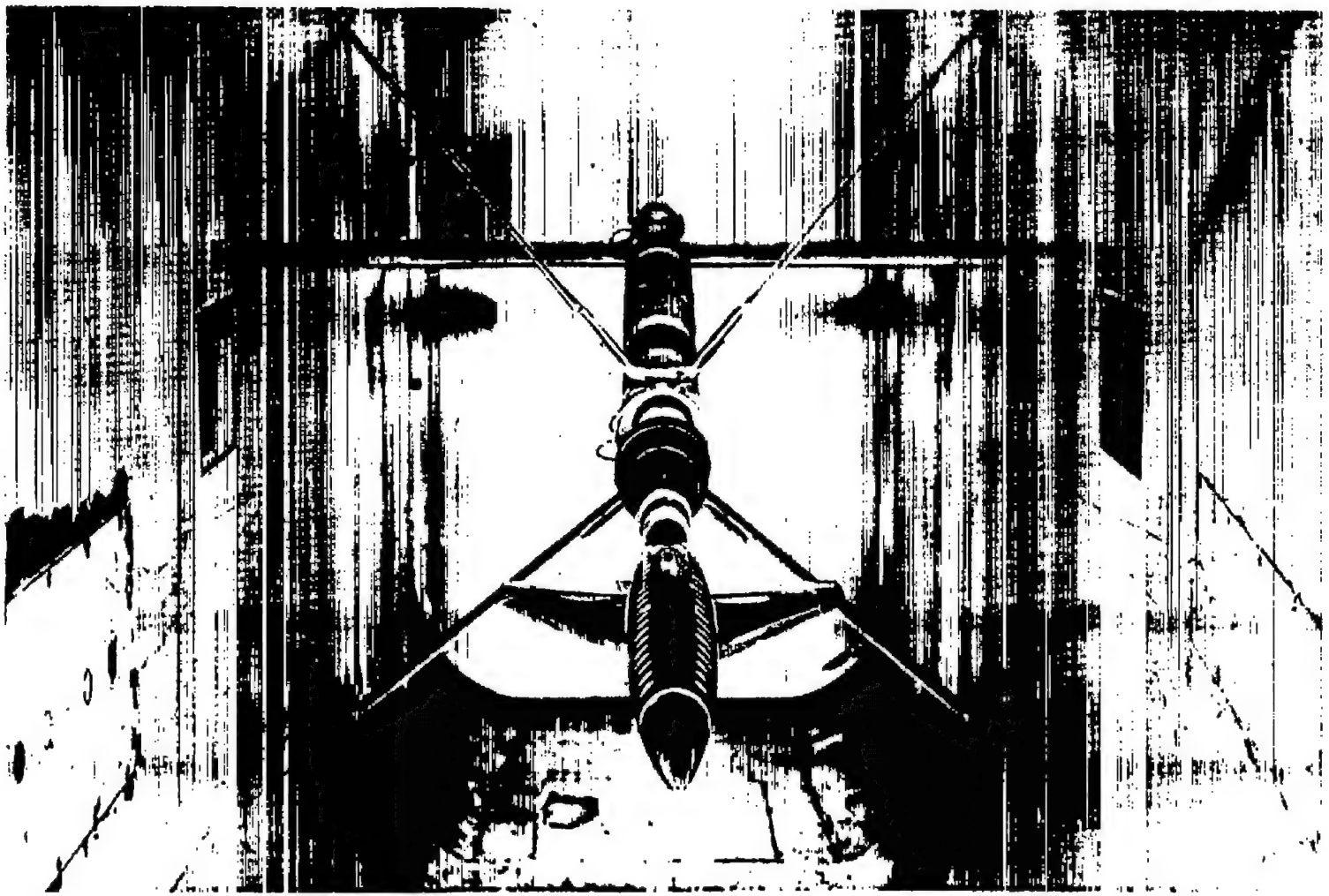

Figure 2.- The clipped-wing configuration mounted in the Langley low-turbulence pressure tunnel. L-76916

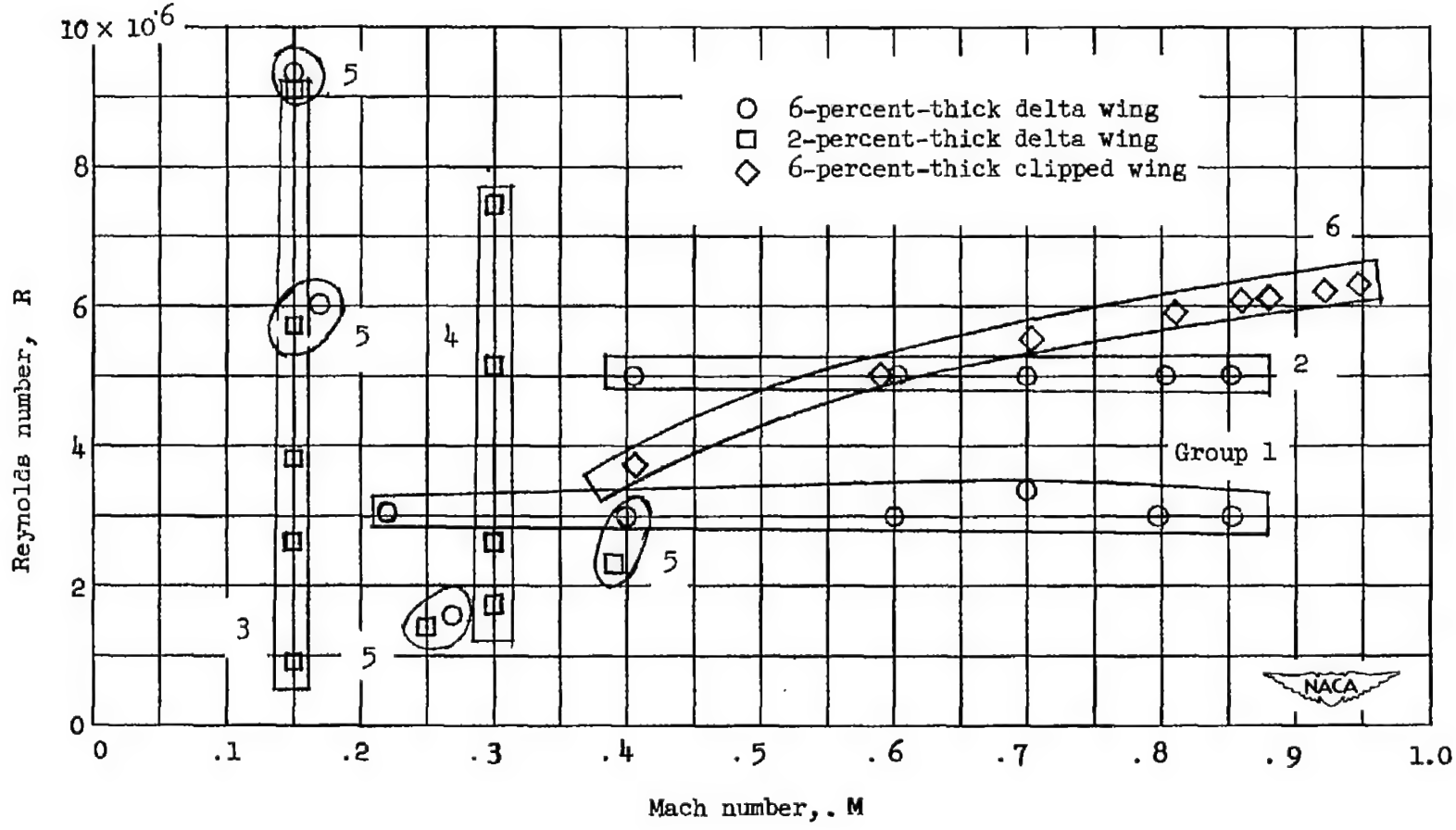

Figure 3.- Range of Mach numbers and Reynolds numbers investigated.

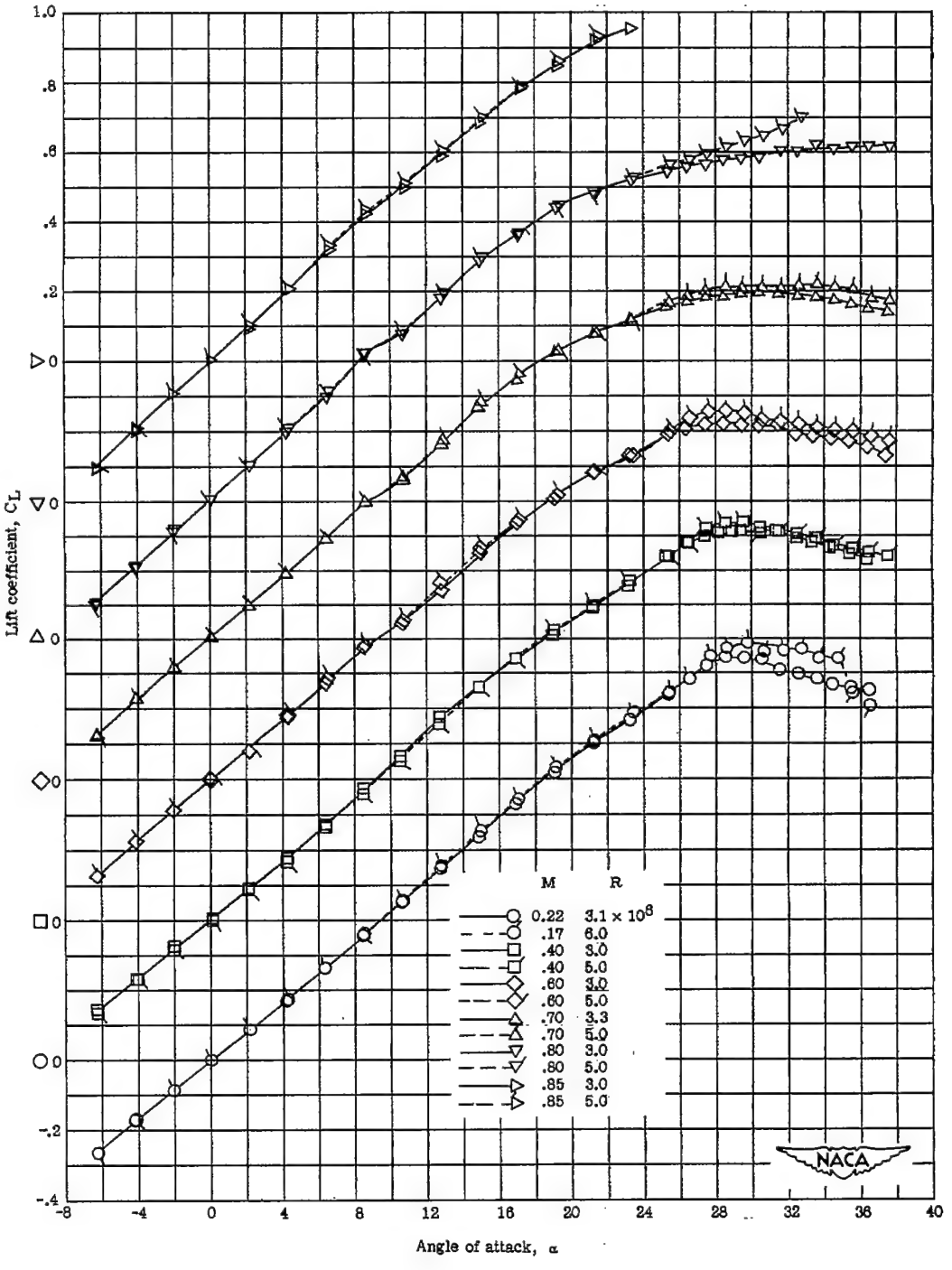

(a) Variation of C_L with α for the wing plus interference.

Figure 4.- Effect of Reynolds number and Mach number on the aerodynamic characteristics of a 6-percent-thick 60° delta wing.

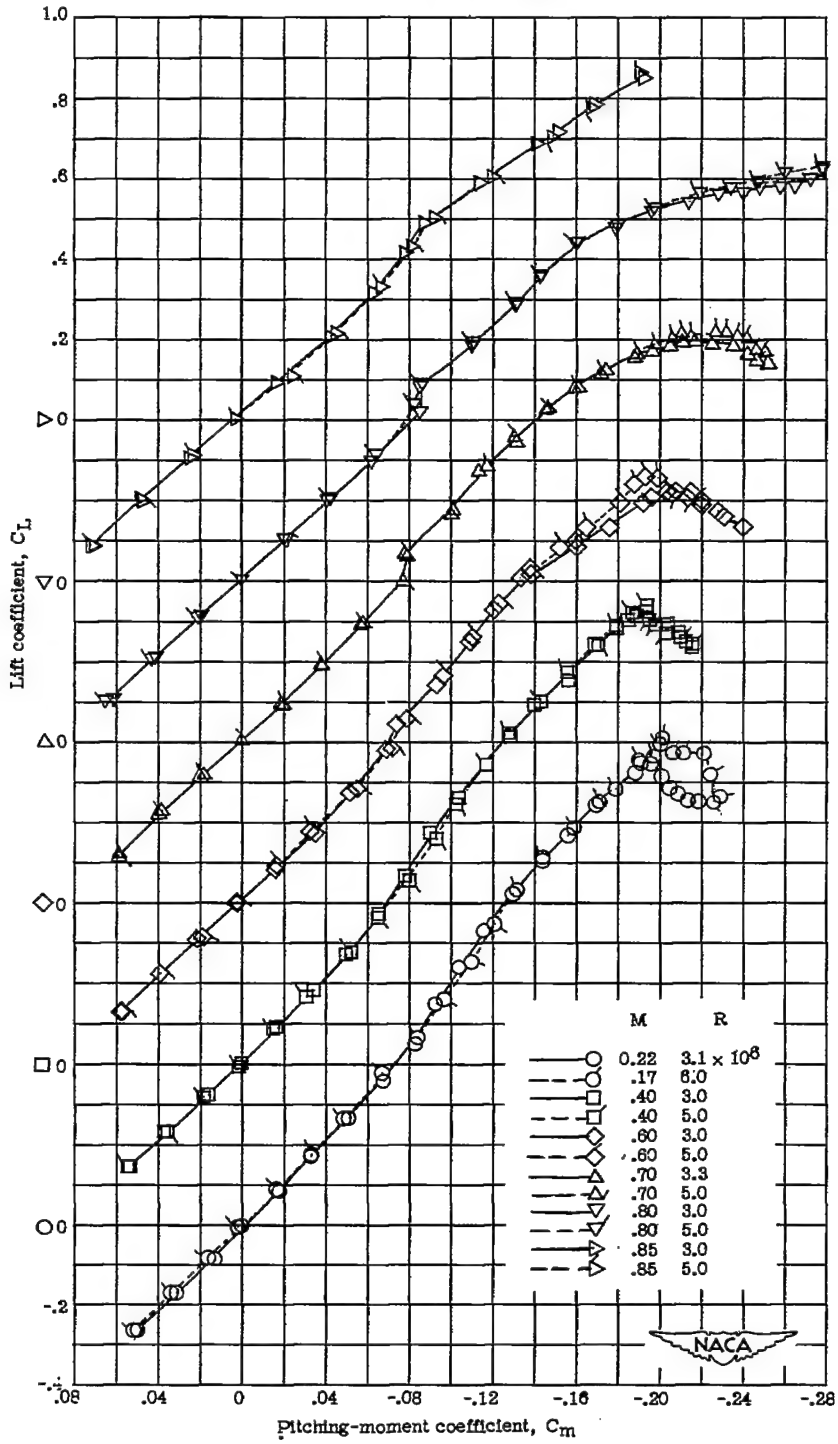

(b) Variation of C_L with C_m for the wing plus interference.

Figure 4.- Continued.

[redacted]

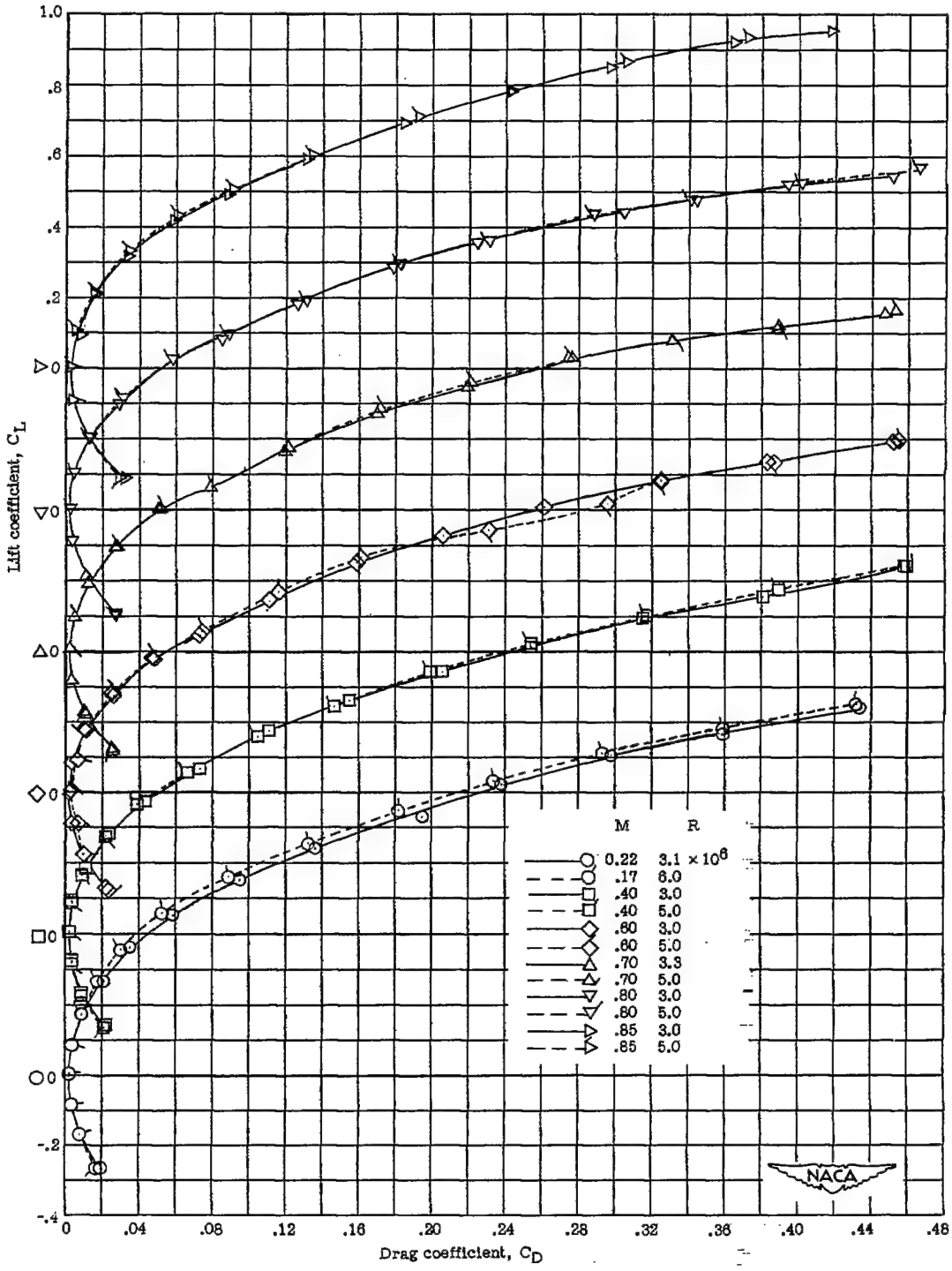

(c) Variation of C_L with C_D for the wing plus interference.

Figure 4.- Continued.

[redacted]

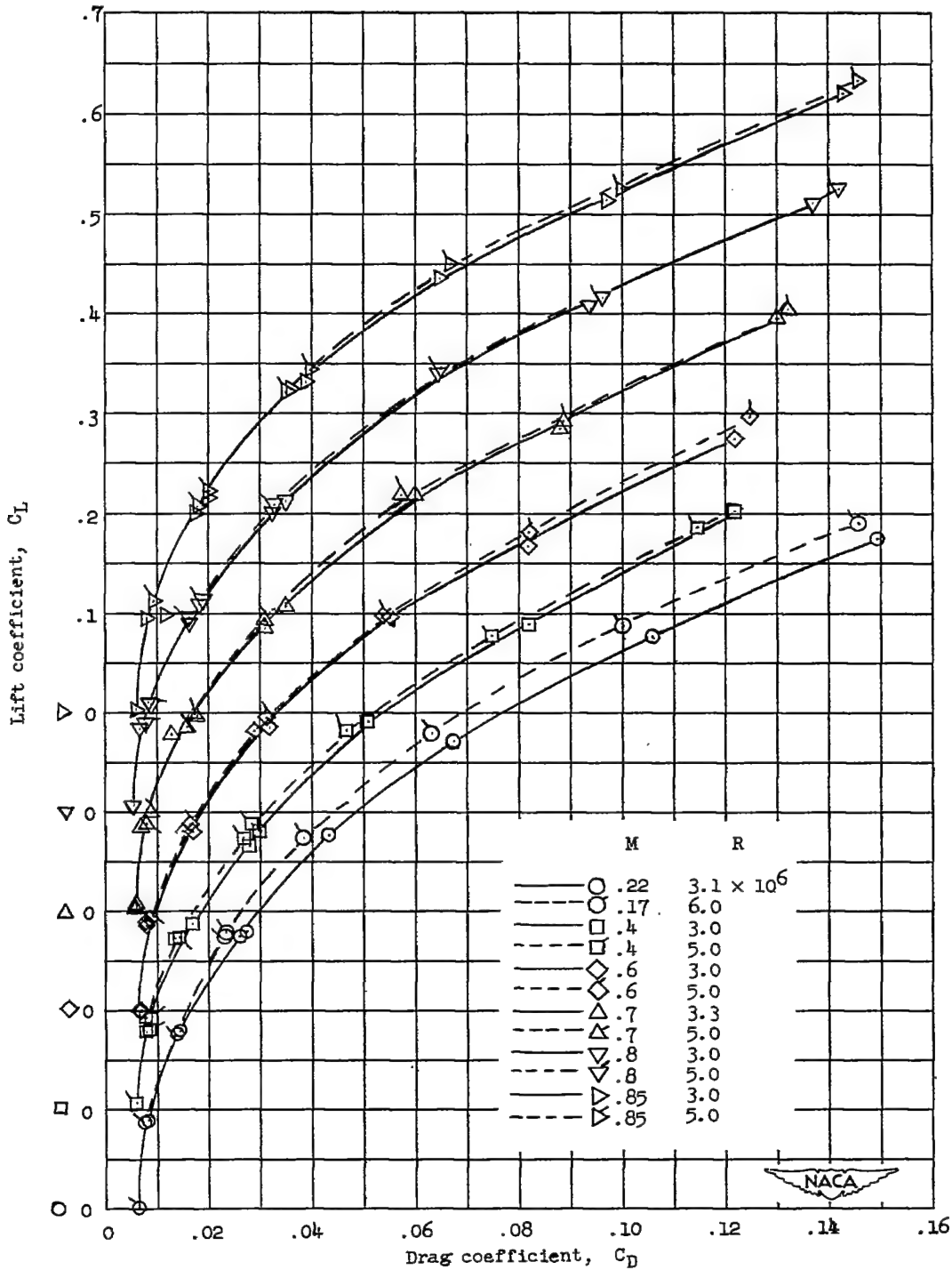

(d) Variation of C_L with C_D for the wing-fuselage configuration.

Figure 4.- Concluded.

[redacted]

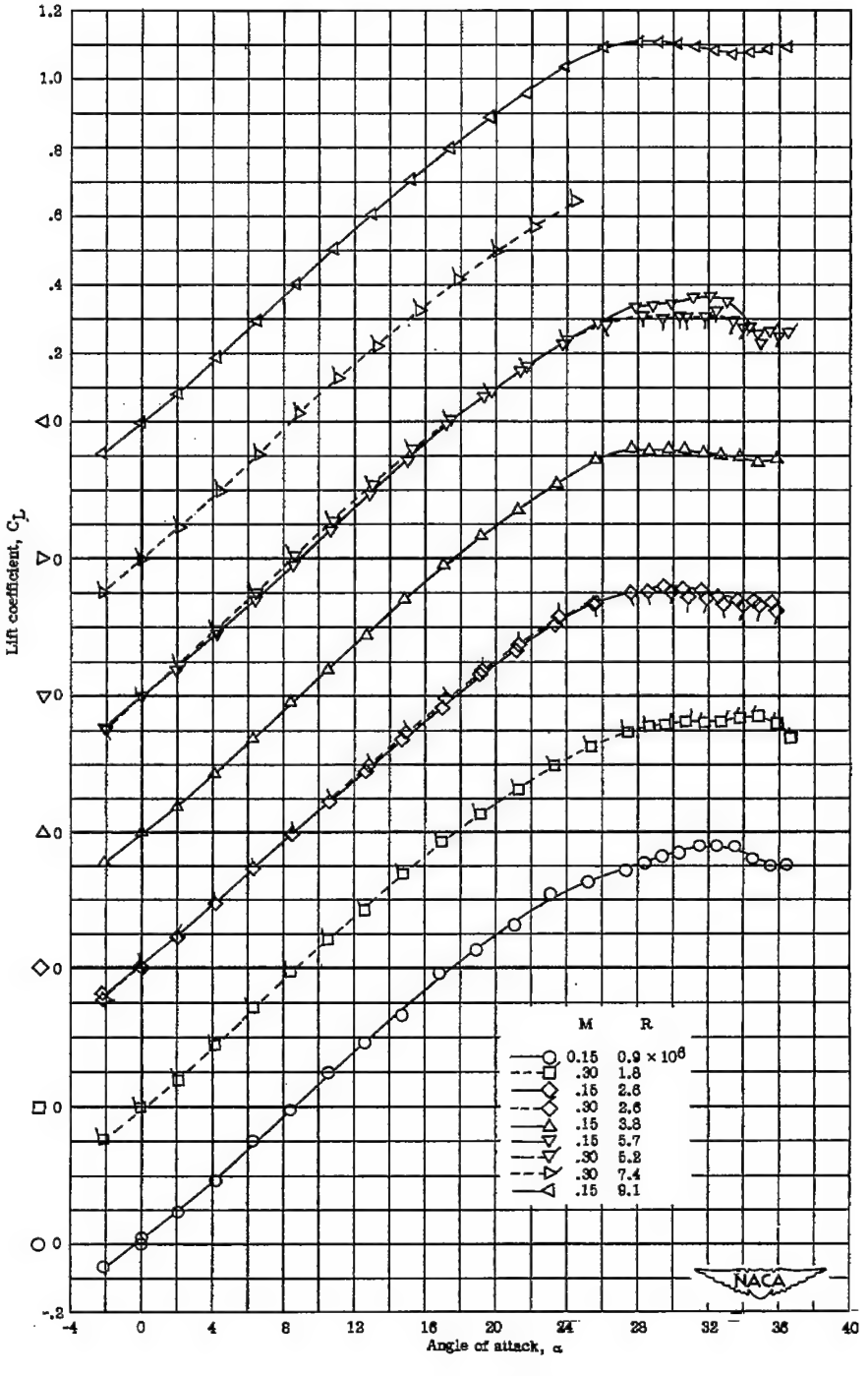

(a) Variation of C_L with α for the wing plus interference.

Figure 5.- Effect of Reynolds number on the aerodynamic characteristics of a 2-percent-thick 60° delta wing at low Mach numbers.

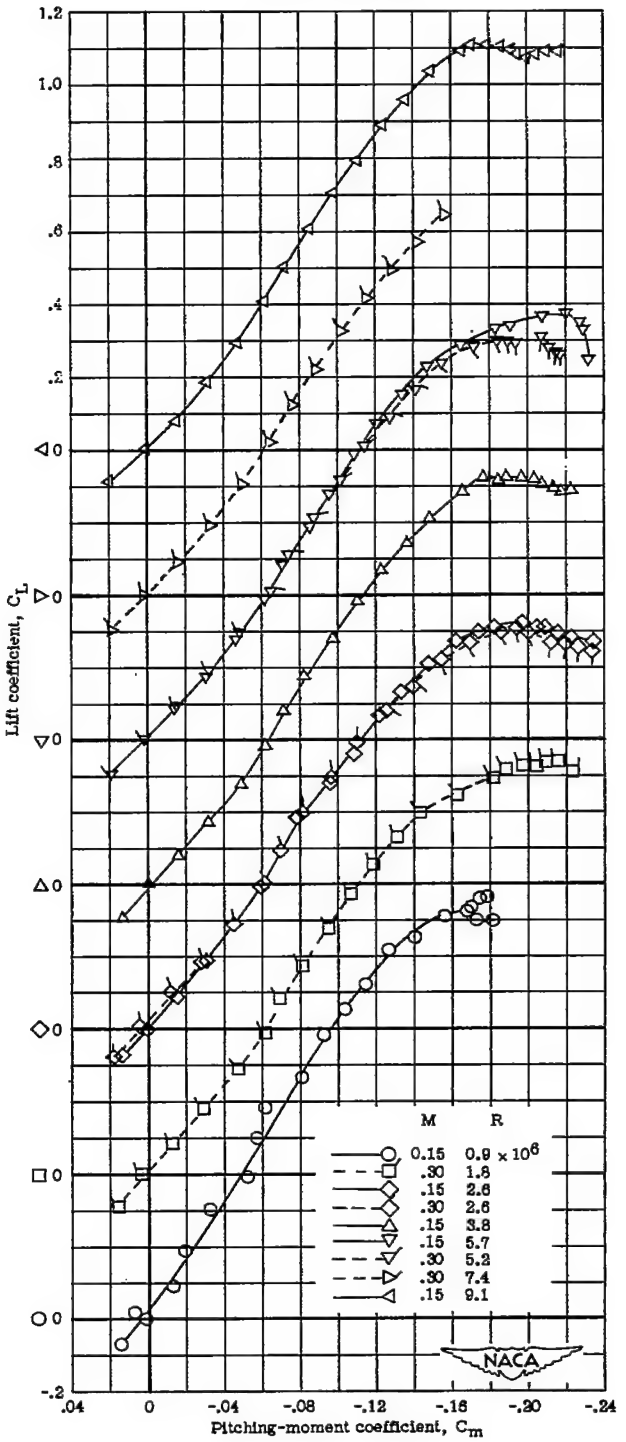

(b) Variation of C_L with C_m for the wing plus interference.

Figure 5.- Continued.

[redacted]

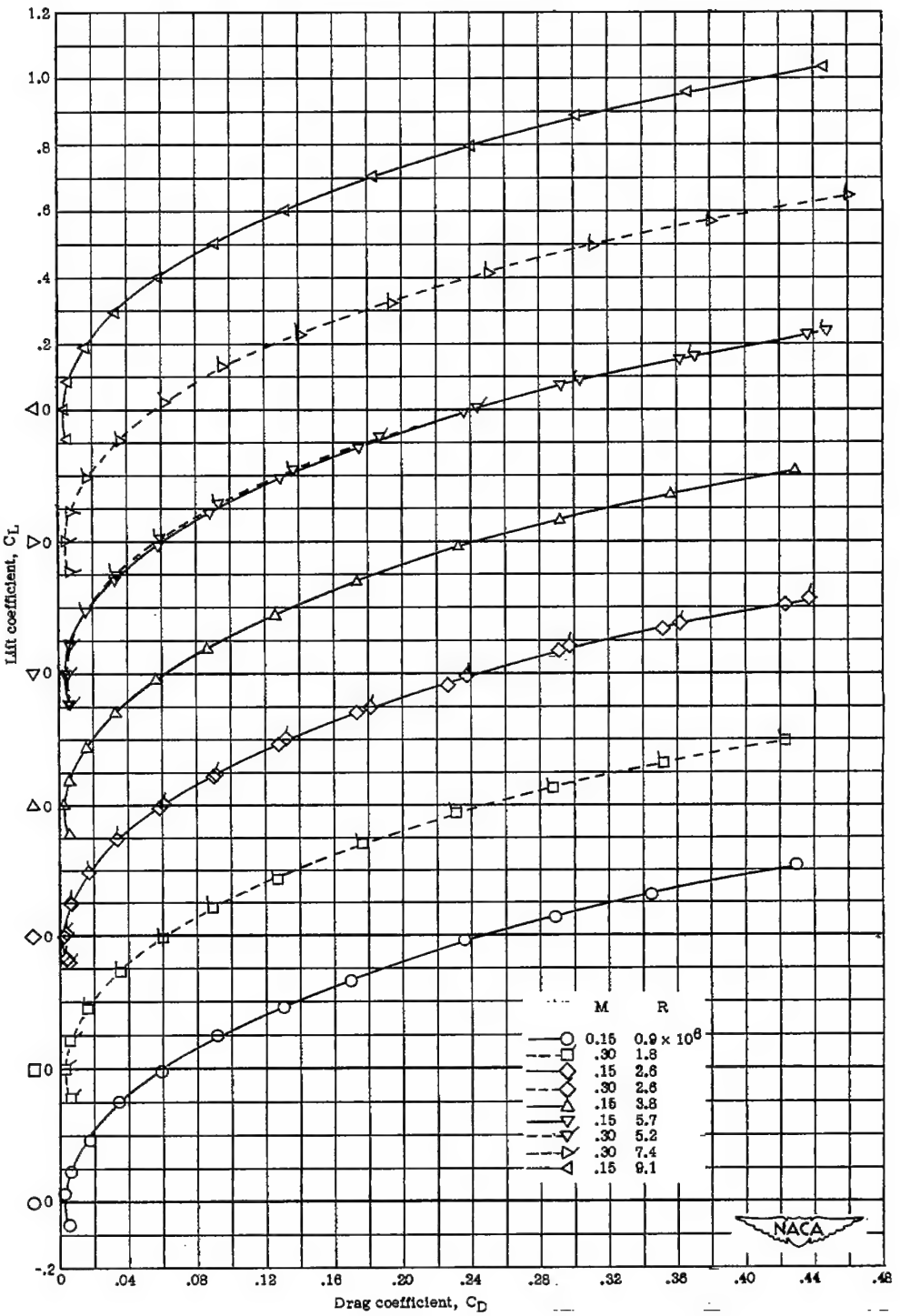

(c) Variation of C_L with C_D for the wing plus interference.

Figure 5.- Continued.

[redacted]

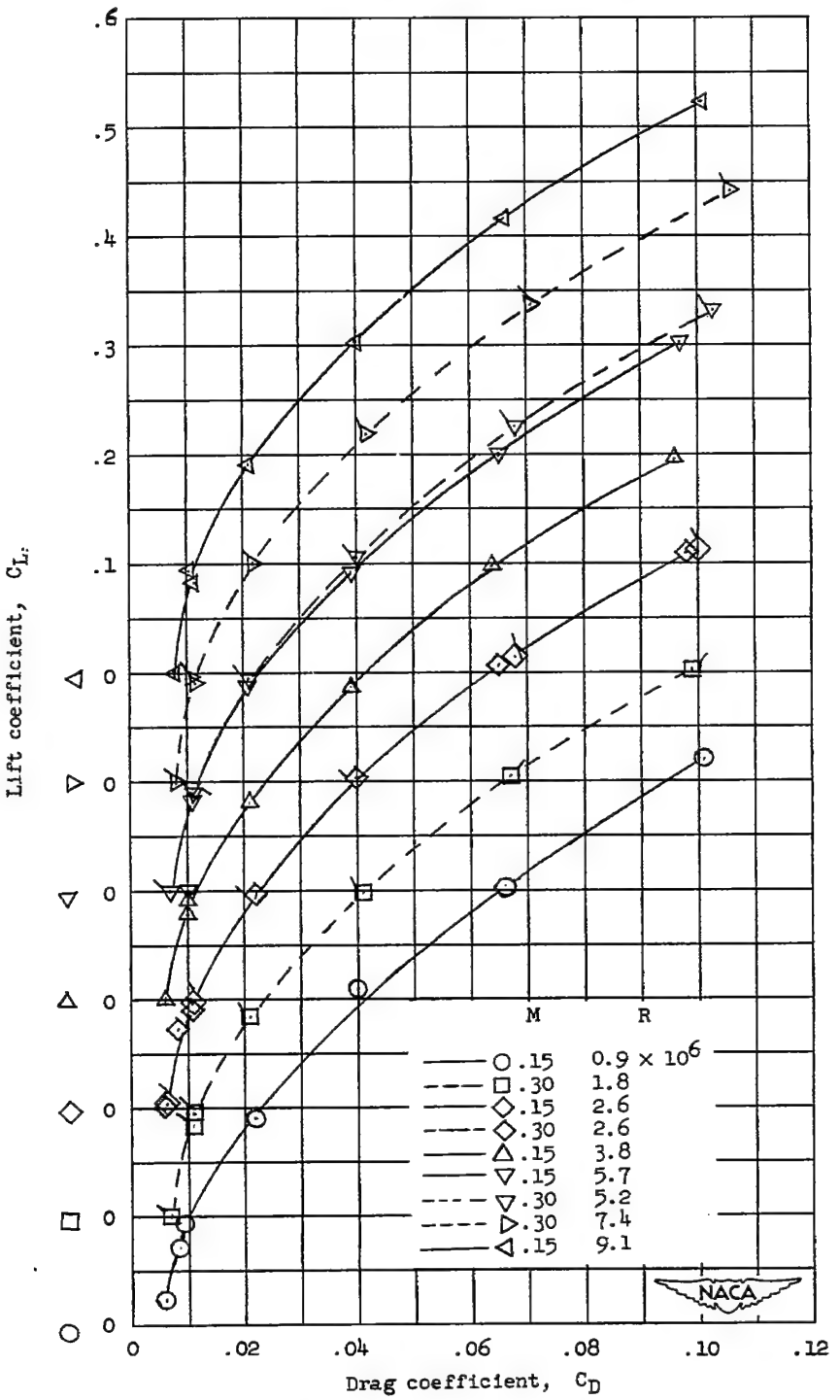

(d) Variation of C_L with C_D for the wing-fuselage configuration.

Figure 5.- Concluded.

[redacted]

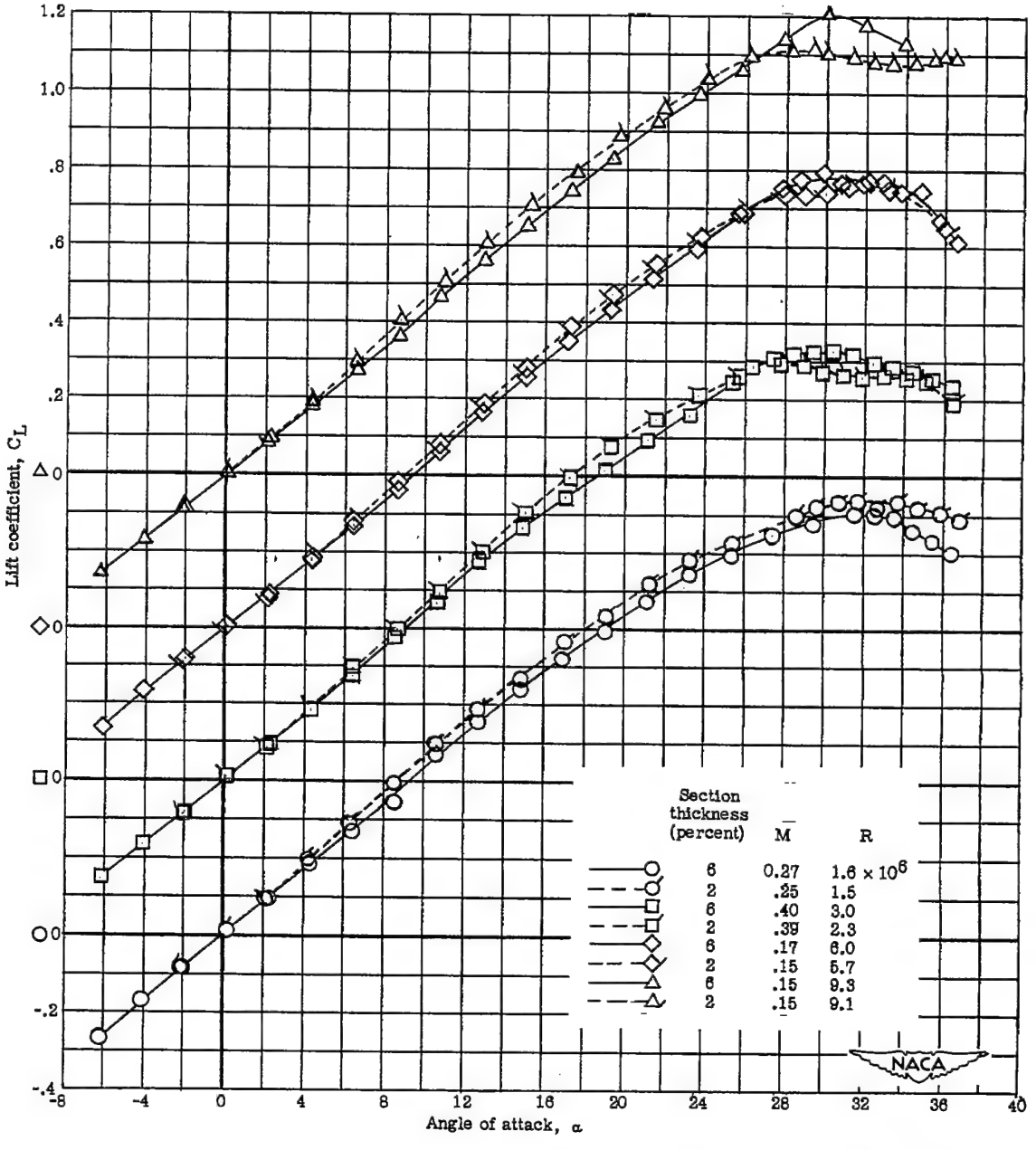

(a) Variation of C_L with α for the wing plus interference.

Figure 6.- Effect of thickness on the aerodynamic characteristics of a 60° delta wing at low Mach numbers.

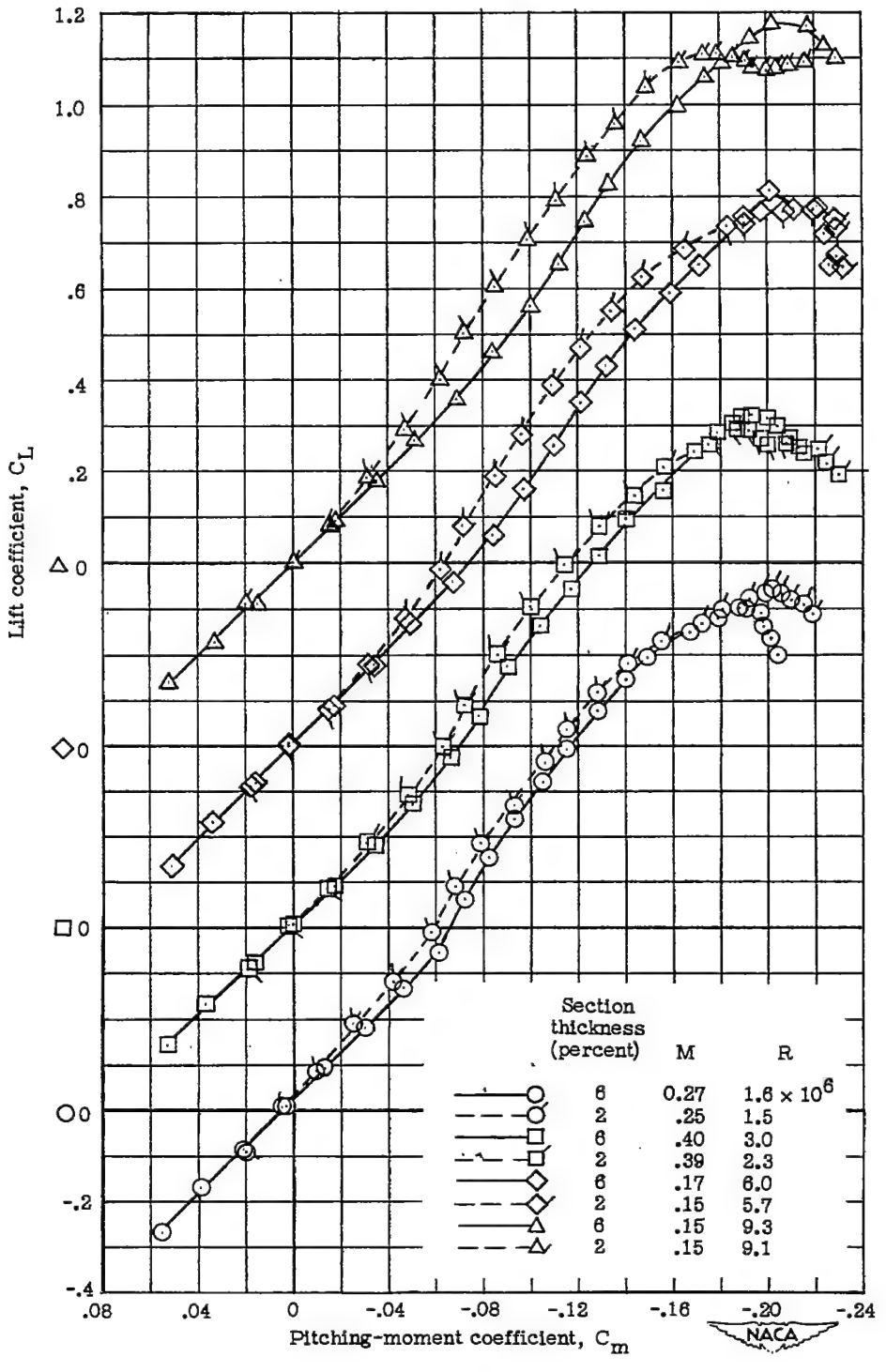

(b) Variation of C_L with C_m for the wing plus interference.

Figure 6.- Continued.

[redacted]

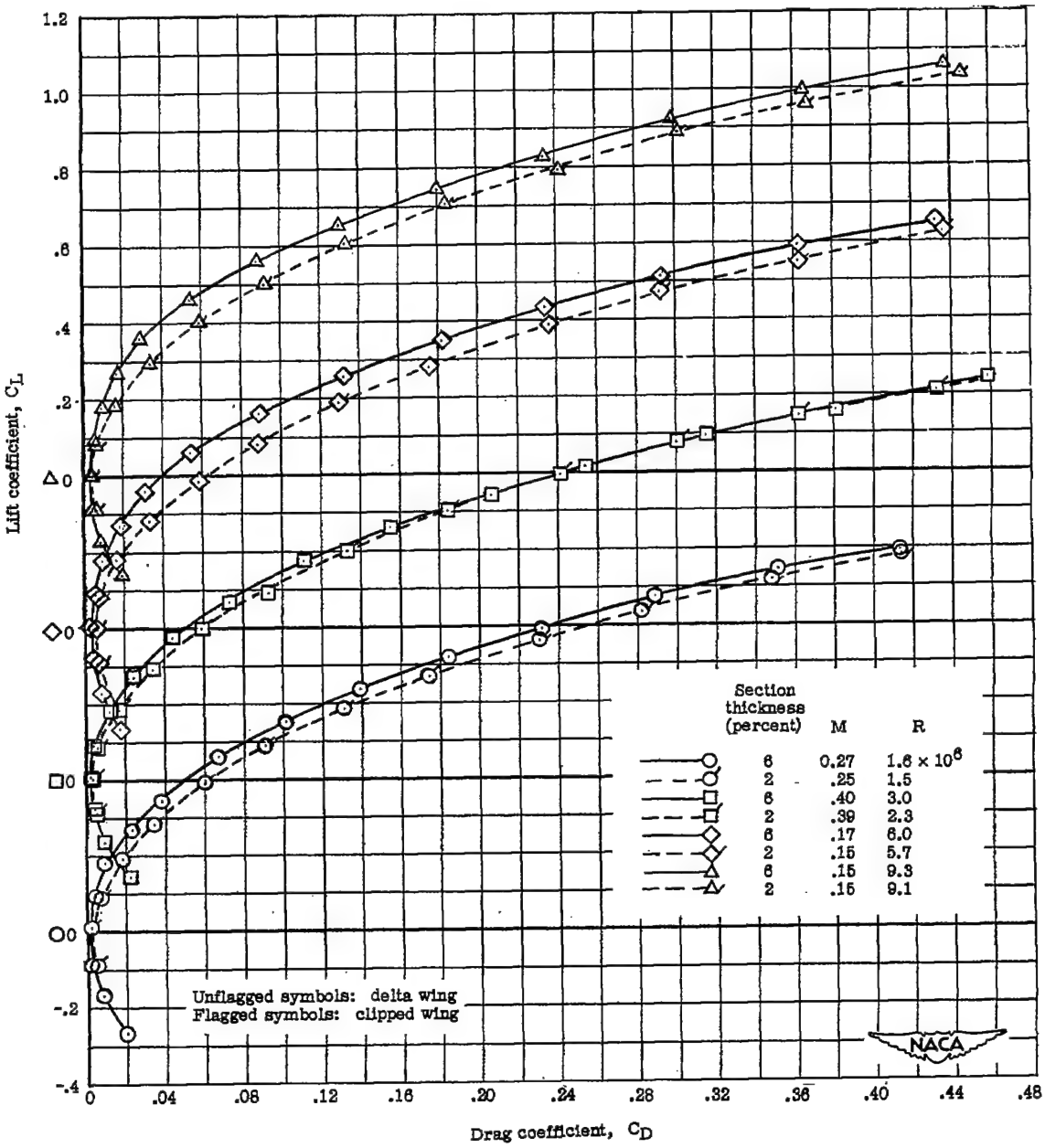

(c) Variation of C_L with C_D for the wing plus interference.

Figure 6.- Continued.

[redacted]

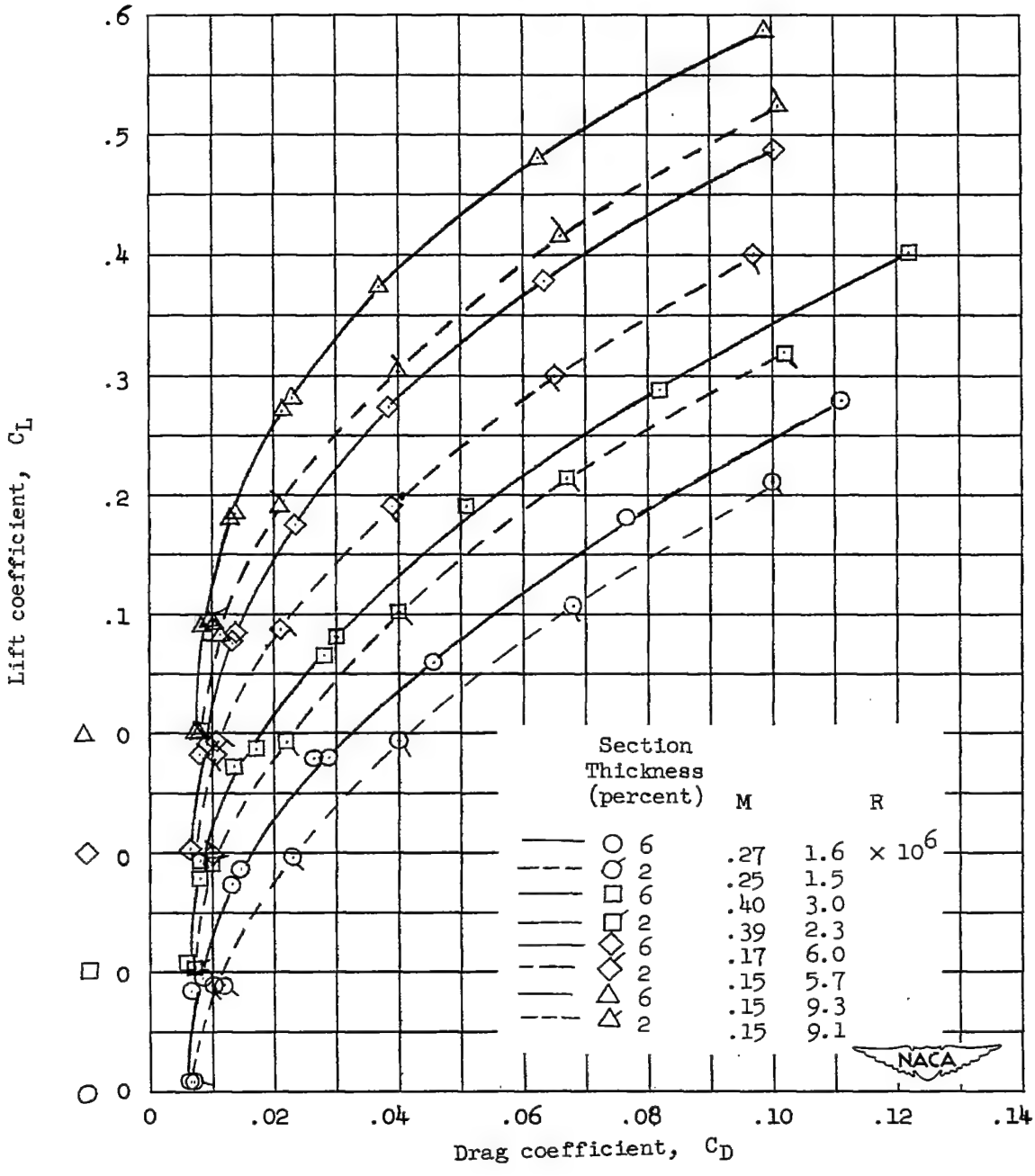

(d) Variation of C_L with C_D for the wing-fuselage configuration.

Figure 6.- Concluded.

[redacted]

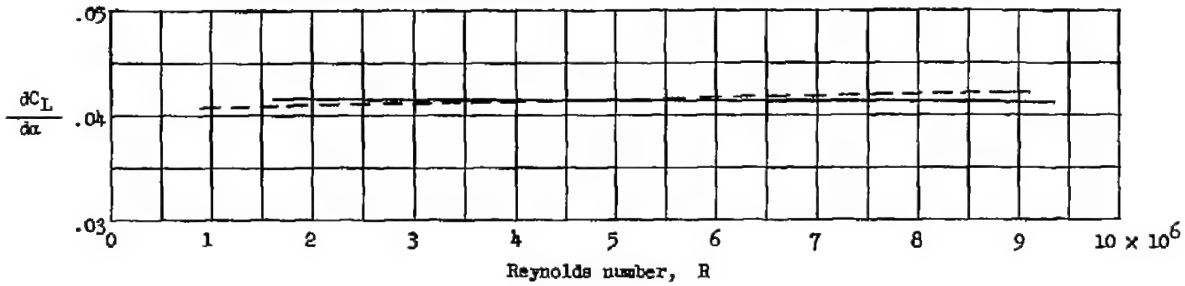

(a) Variation of $dC_L/d\alpha$ with Reynolds number at Mach numbers less than 0.3.

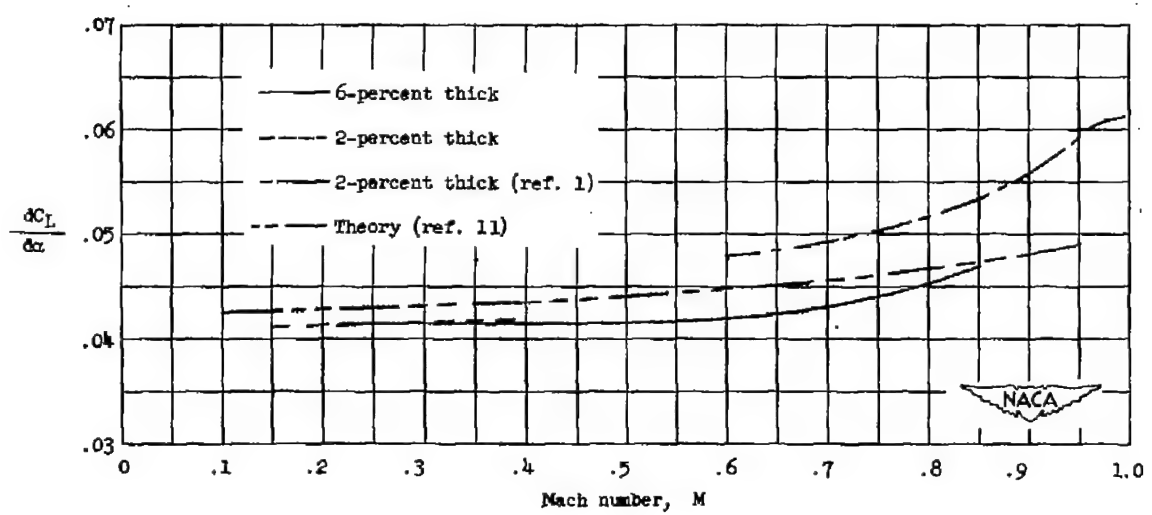

(b) Variation of $dC_L/d\alpha$ with Mach number at Reynolds number of approximately 3×10^6.

Figure 7.- Effect of thickness on $dC_L/d\alpha$ measured at zero lift for the wing plus interference.

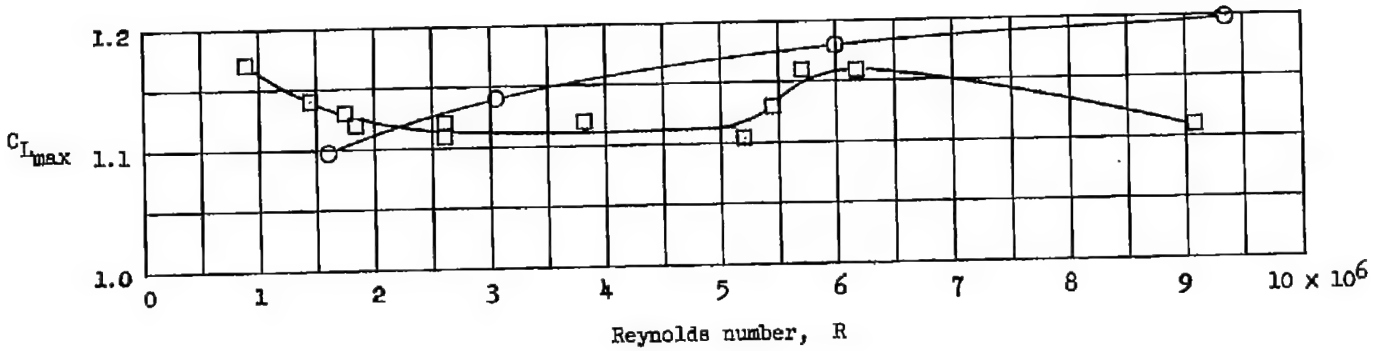

(a) Variation of $C_{L_{max}}$ with Reynolds number at Mach numbers less than 0.3.

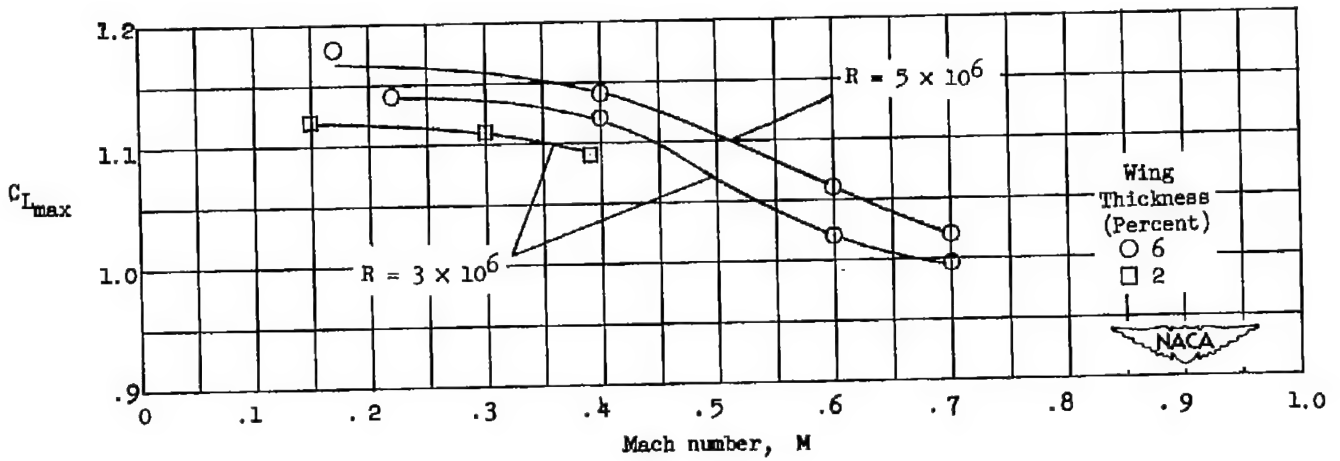

(b) Variation of $C_{L_{max}}$ with Mach number.

Figure 8.- Effect of thickness on $C_{L_{max}}$ for the wing plus interference.

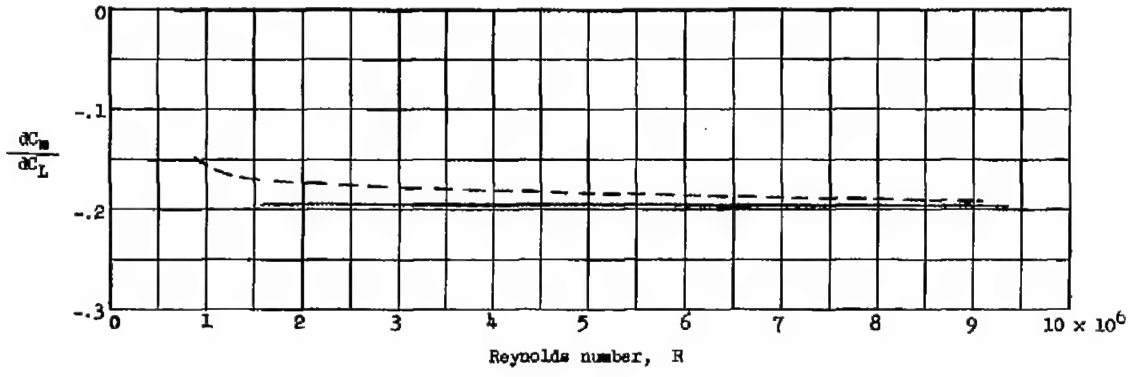

(a) Variation of dC_m/dC_L with Reynolds number at Mach numbers less than 0.3.

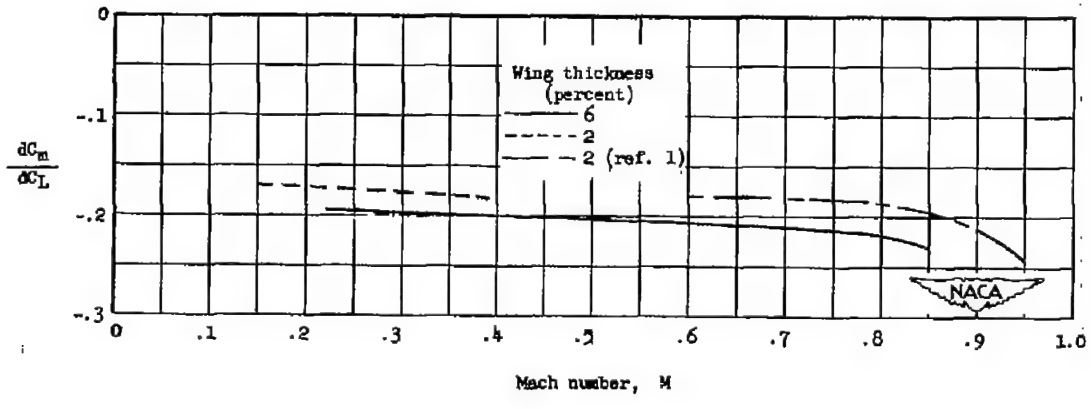

(b) Variation of dC_m/dC_L with Mach number at Reynolds number of approximately 3×10^6.

Figure 9.- Effect of thickness on dC_m/dC_L measured at zero lift for the wing plus interference.

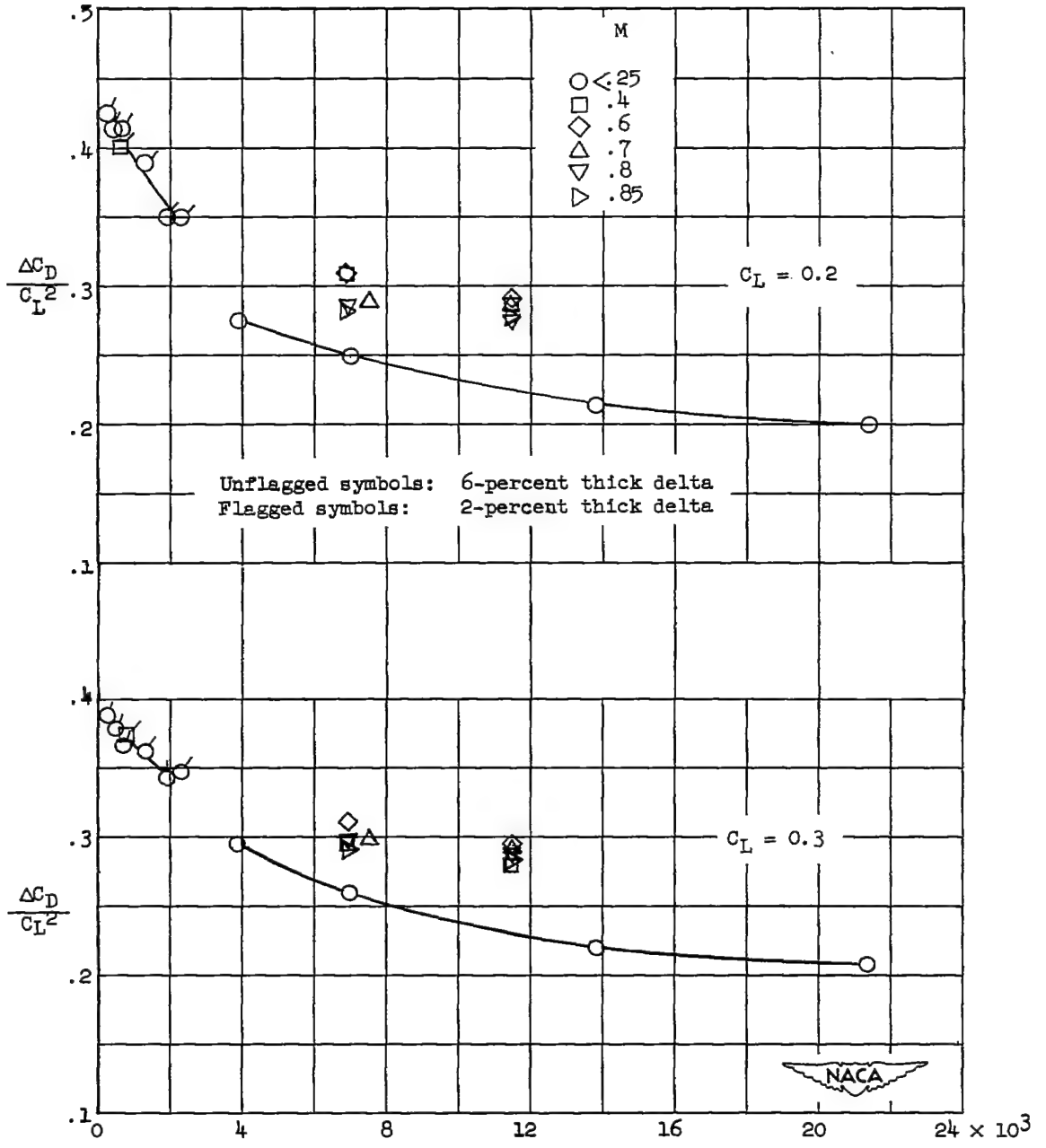

Figure 10.- Effect of Reynolds number on drag due to lift of the wing-fuselage configuration.

[redacted]

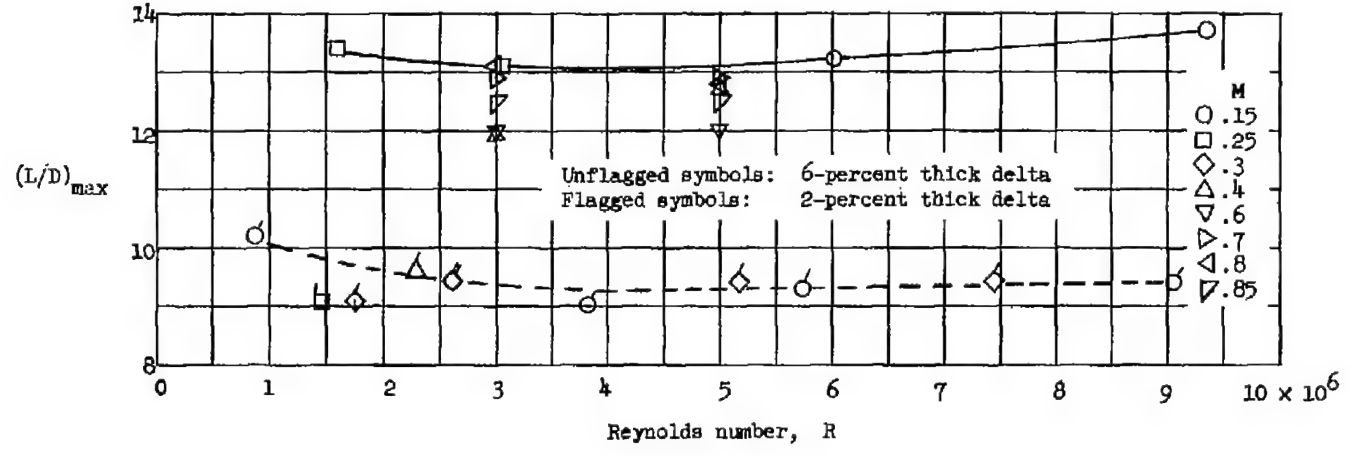

(a) Variation of $(L/D)_{max}$ with Reynolds number.

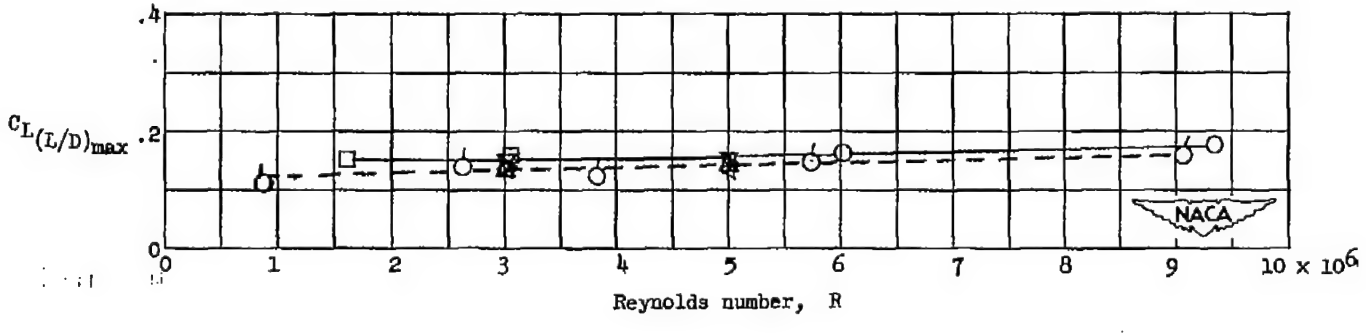

(b) Variation of $C_{L_{(L/D)_{max}}}$ with Reynolds number.

Figure 11.- Effect of thickness on $(L/D)_{max}$ and $C_{L_{(L/D)_{max}}}$ of the wing-fuselage configuration.

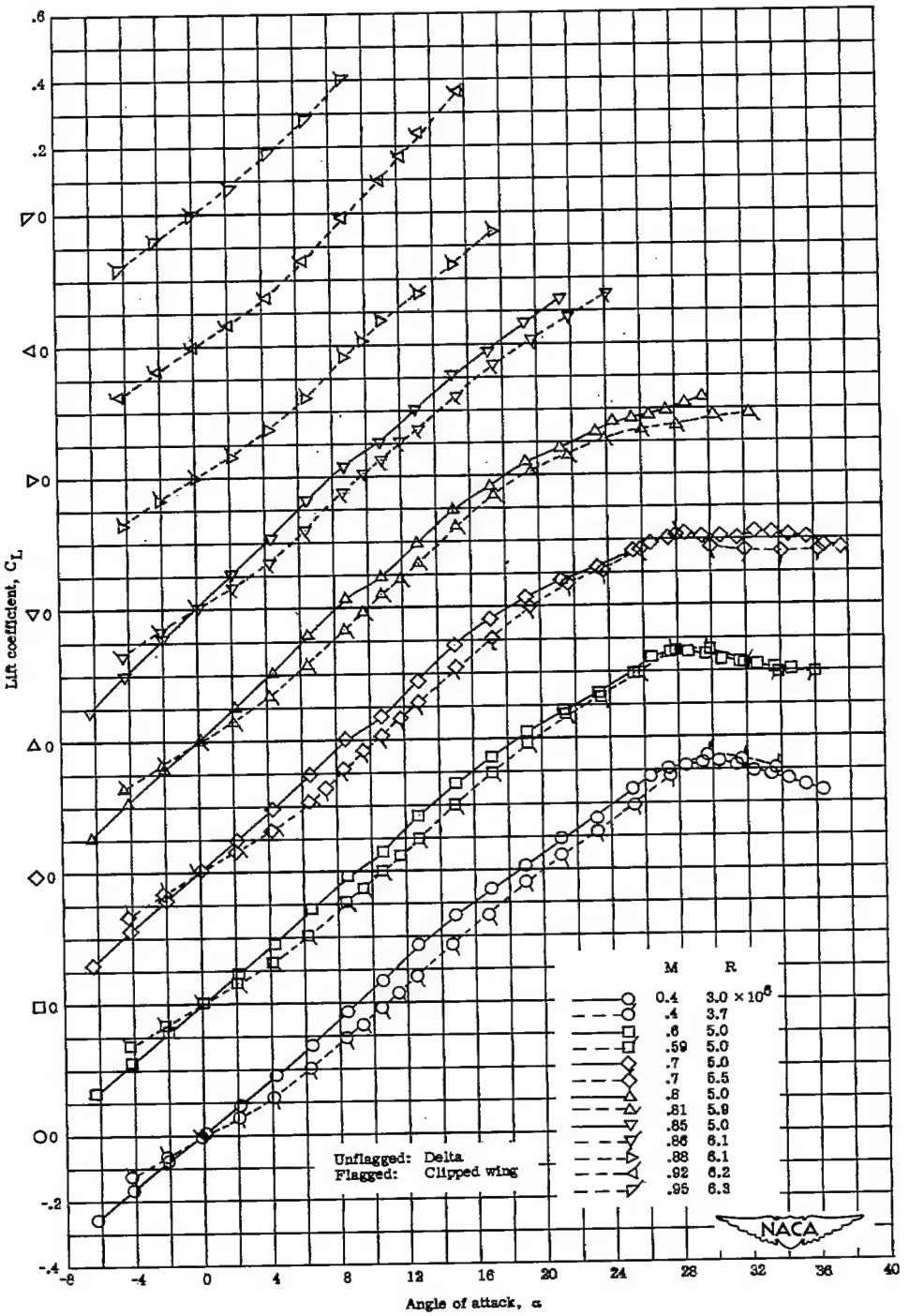

(a) Variation of C_L with α for the wing plus interference.

Figure 12.- Effect of removal of the pointed tips on the aerodynamic characteristics of a 6-percent-thick 60° delta wing.

[redacted]

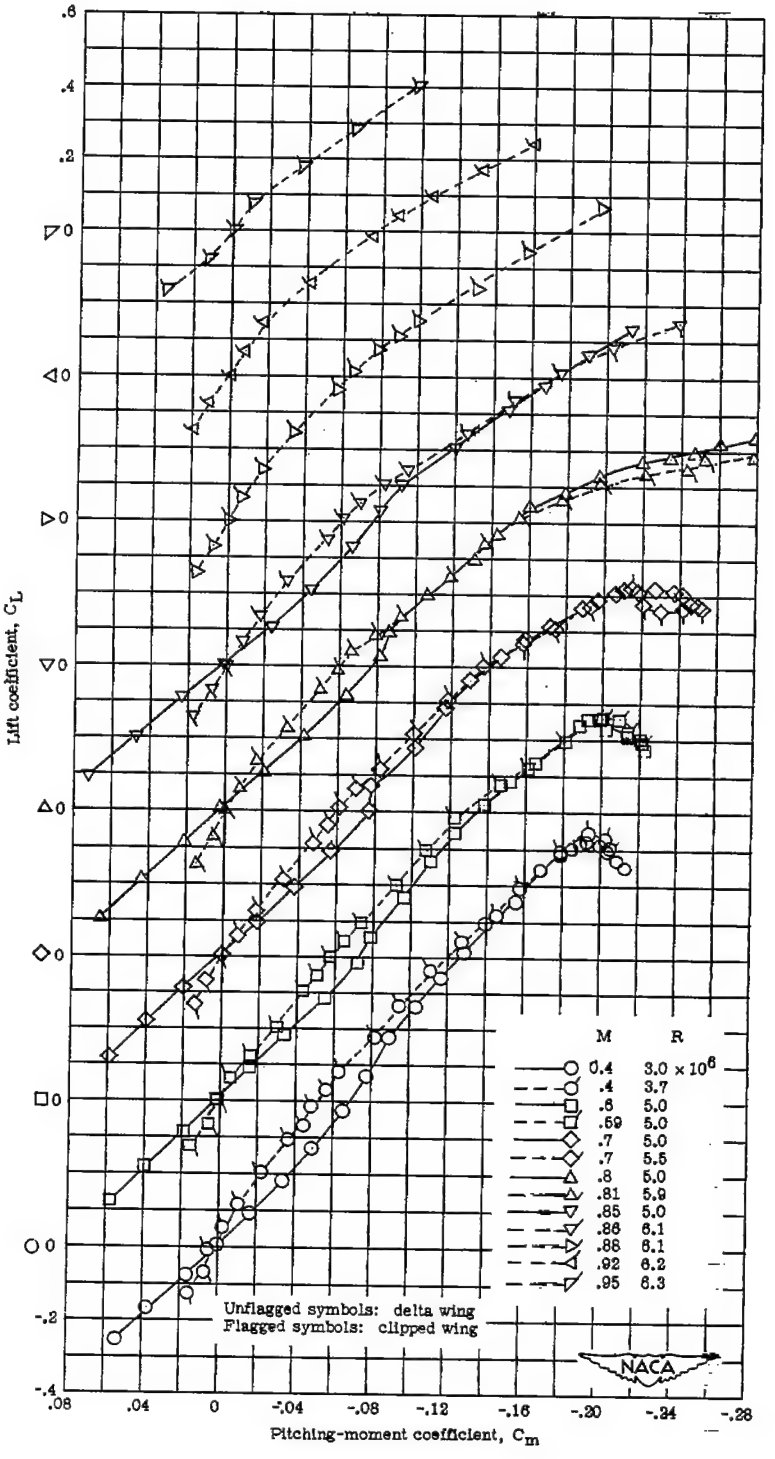

(b) Variation of C_L with C_m for the wing plus interference.

Figure 12.- Continued.

[redacted]

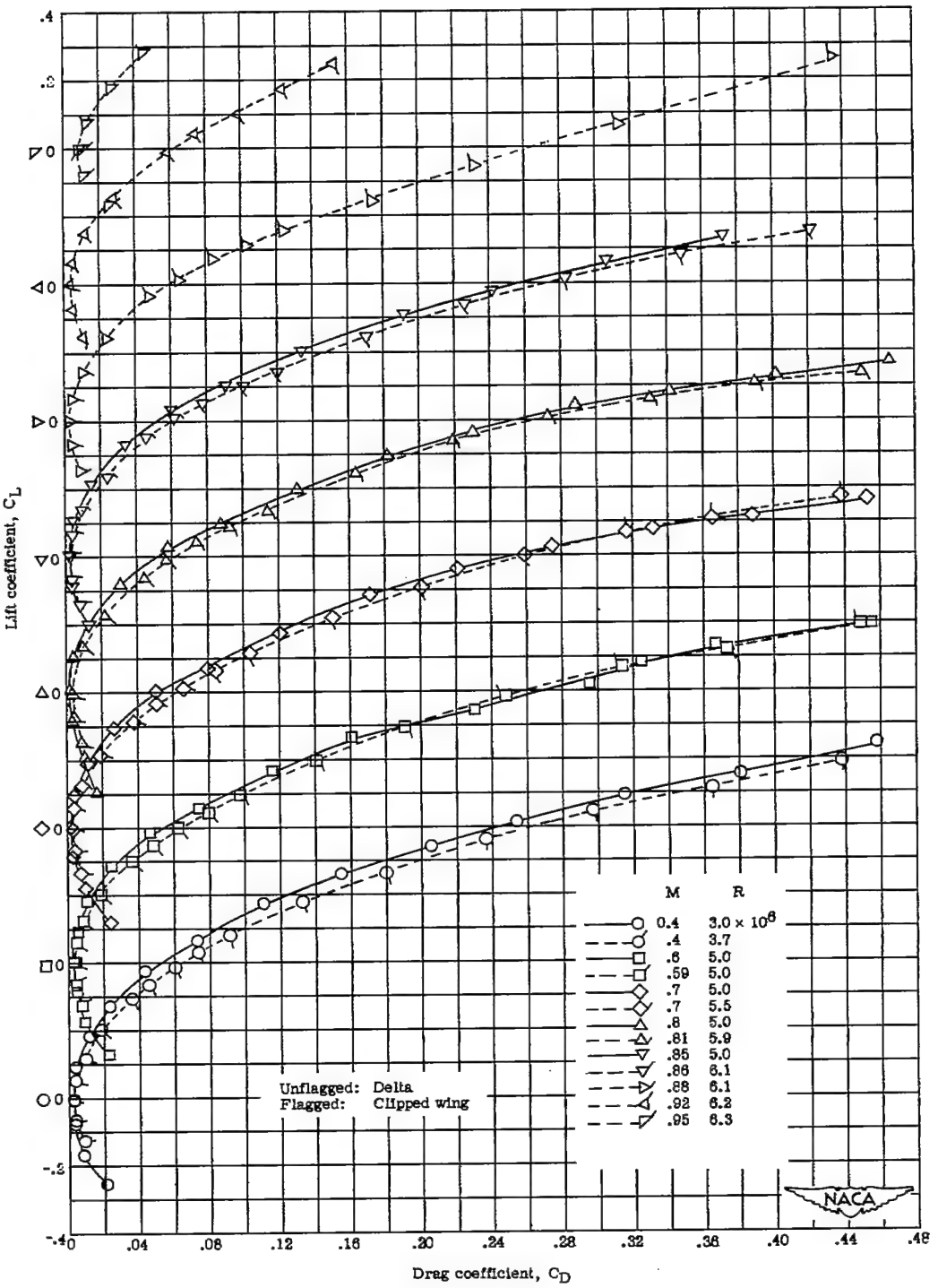

(c) Variation of C_L with C_D for the wing plus interference.

Figure 12.- Continued.

[redacted]

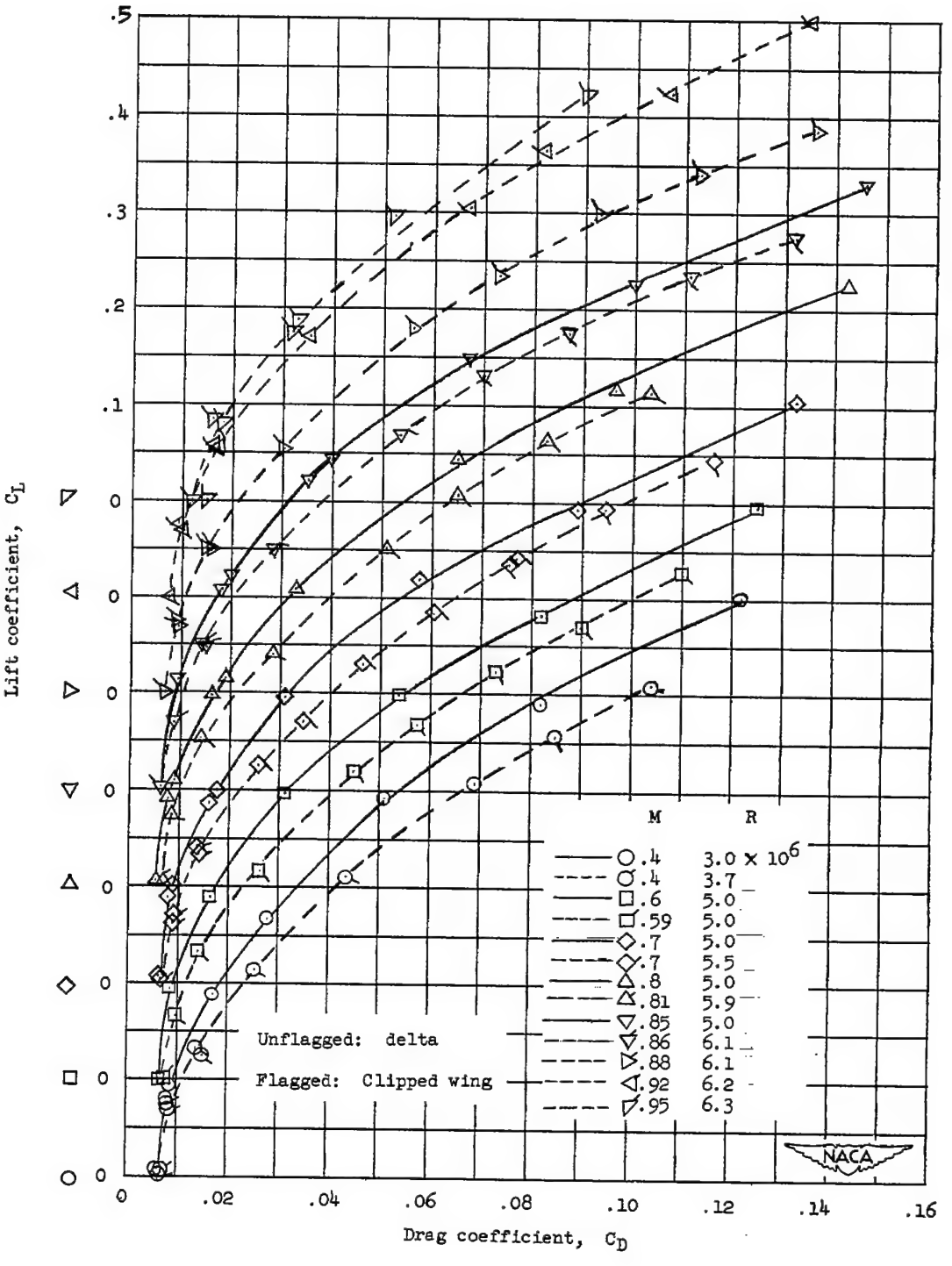

(d) Variation of C_L with C_D for the wing-fuselage configurations.

Figure 12.- Concluded.

[redacted]

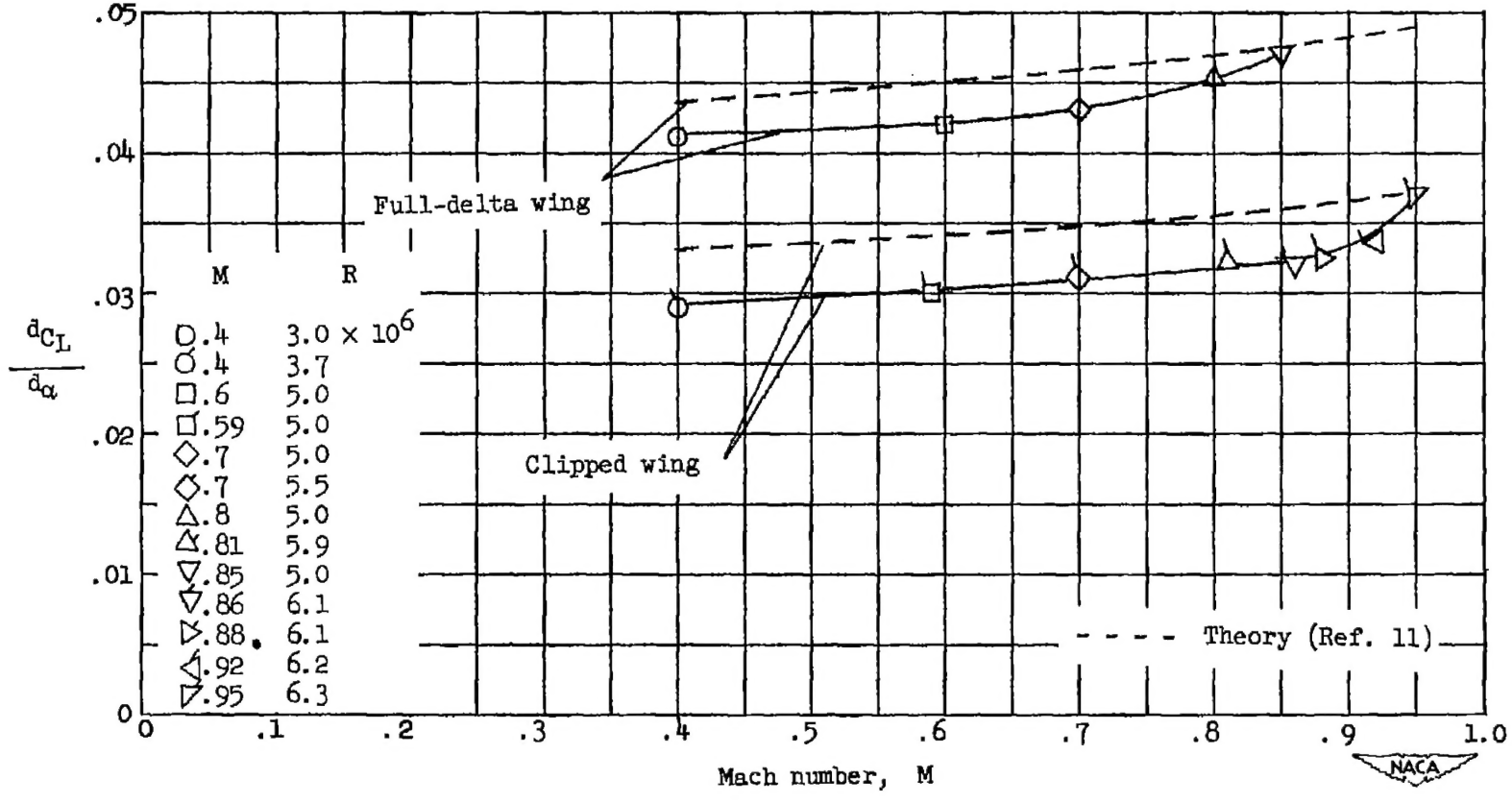

Figure 13.- Effect of removing the tips on $dC_L/d\alpha$ for the wing plus interference.

M	R
.4	3.0×10^6
.4	3.7
.6	5.0
.59	5.0
.7	5.0
.7	5.5
.8	5.0
.81	5.9
.85	5.0
.86	6.1
.88	6.1
.92	6.2
.93	6.3

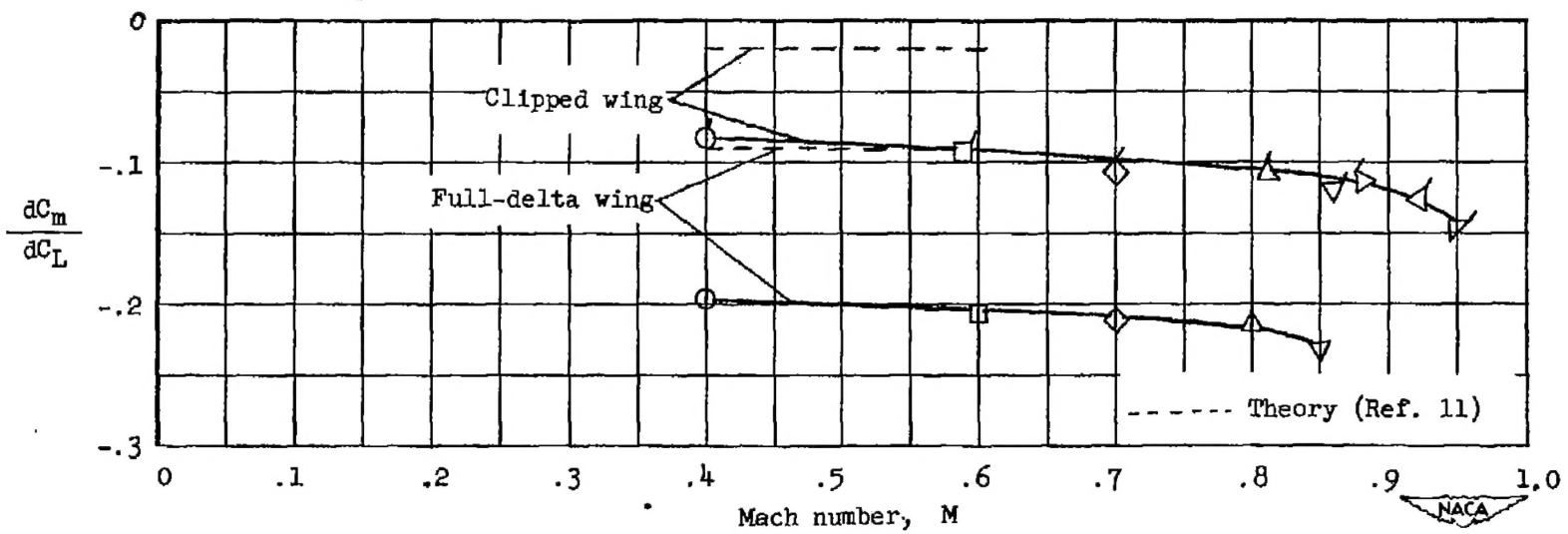

Figure 14.- Effect of removing the tips on dC_m/dC_L measured at zero lift for the wing plus interference.

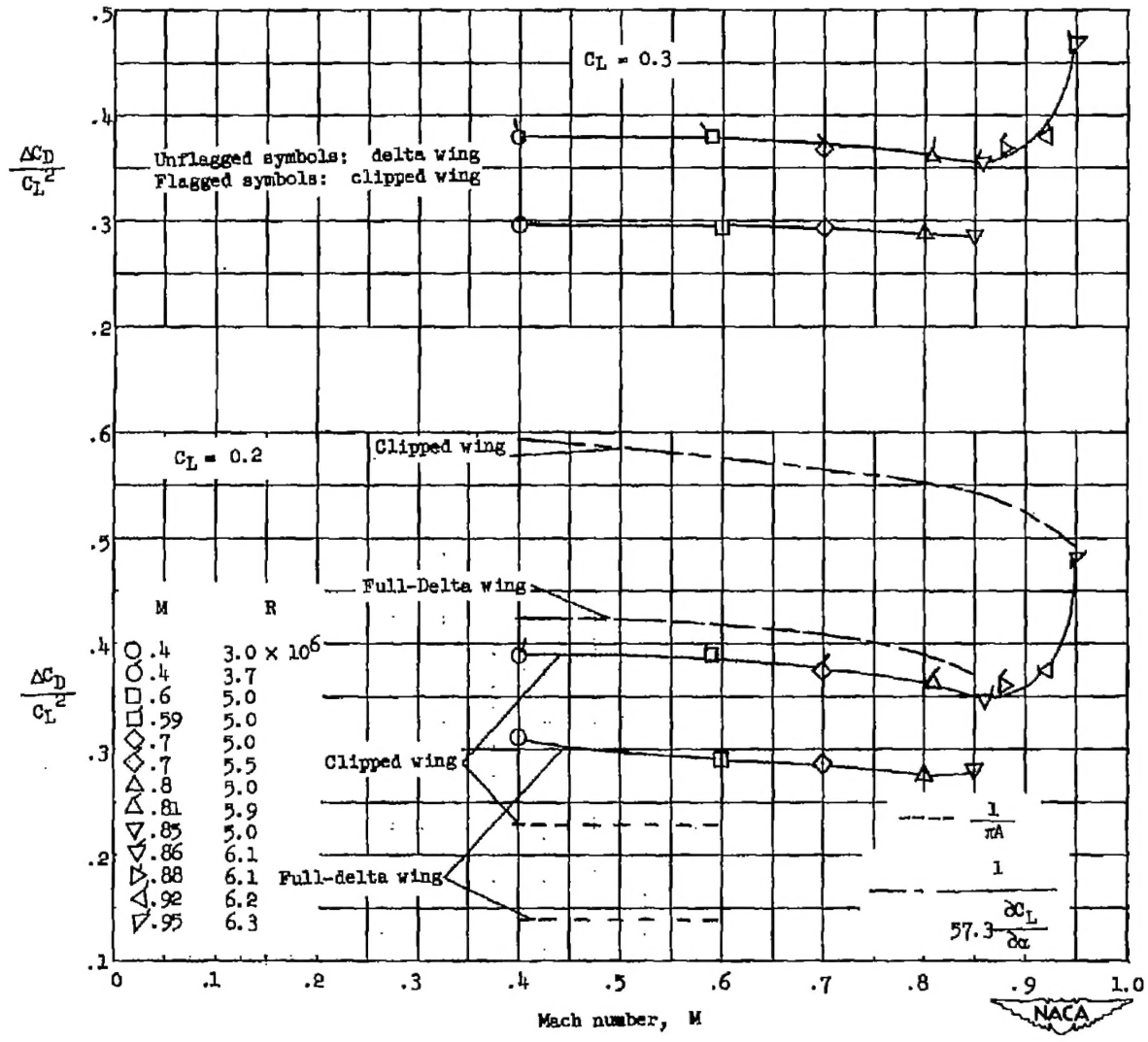

Figure 15.- Effect of removing the tip on drag due to lift of the wing-fuselage configuration at C_L = 0.2 and 0.3.

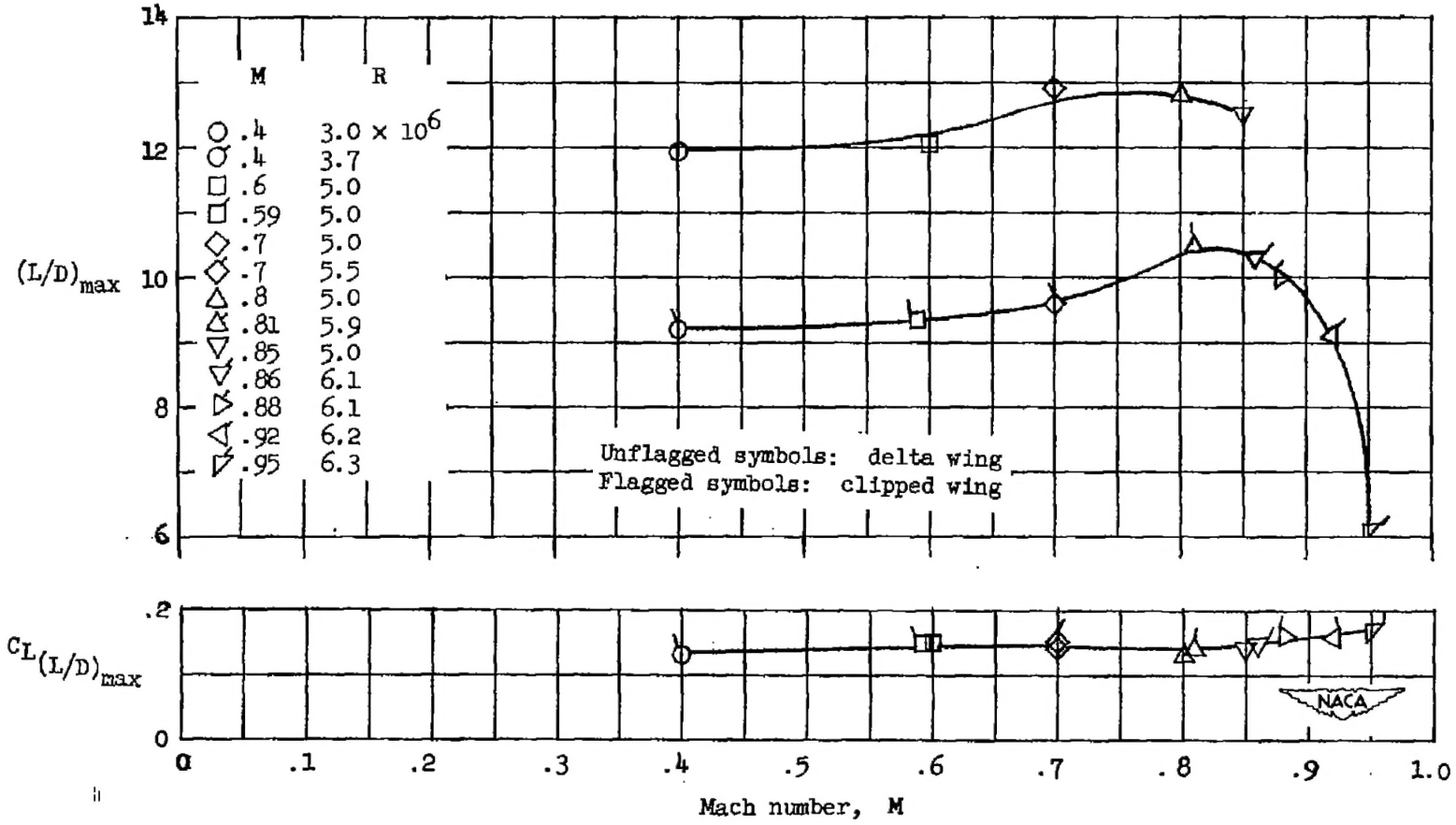

Figure 16.- Effect of removing the tips on $(L/D)_{max}$ and $C_{L_{(L/D)_{max}}}$ of the wing-fuselage configuration.